

# Quantifying flood risk reduction strategies for Tirana

S.P.C. Suijkens



# Quantifying flood risk reduction strategies for Tirana

by

S.P.C. Suijkens

Additional Thesis  
Delft University of Technology

Student number: 1382276  
Supervisors: Dr. D. Wüthrich, TU Delft  
Dr. Ir. M.M. Rutten, TU Delft

The cover picture provides an areal view of the extent of flooding in Albania (Davies, 2017).

# Abstract

Global economic losses due to flooding have increased over the last 50 years, with damages estimated in the billions of dollar each year. Governmental institutions face great challenges to reduce flood risk under the influence of population increase, urbanization and climate change. Interdisciplinary urban planning becomes more important to mitigate flood risk with a multidisciplinary approach and insights in conceptual designs is important to support interdisciplinary cooperation.

An example of a country facing great challenges is Albania, where on average 23 flooding events occur each year and at least 54% of the regions have been affected. In addition, the country faces challenges in the disciplines of urban planning, transport and water quality. The capital city Tirana and surroundings were highly affected by flooding events in 2017. The city is prone to flash floods and, especially in the winter months, river flooding. It is crucial to identify areas susceptible to flooding and to quantify the impact on flood risk reduction of potential measures. Data availability imposes a major constraint to quantify flood risk in urban areas with currently available assessment methods. Therefore a flood risk assessment method needs to be identified that is applicable in areas with poor or scarce data. Once the method is identified it can be applied in the Tirana region to identify flood risk and to quantify the impact of measures. Potential measures were developed in an interdisciplinary workshop with students from the TU Delft and Tirana and focussed on the Tirana region, including the Lana river area. The proposed measures for the Lana river are quantified in the risk assessment in this thesis.

The identified method defines flood risk as the product of hazard, exposure and vulnerability expressed in Expected Annual Damage (EAD) in Euro. European depth-damage functions for four land use classes are used, in combination with maximum damage values, to express the exposure and vulnerability component. The hazard is described by inundation maps and the development forms the core of this thesis. With the use of a Digital Elevation Model (DEM) a Height Above Nearest Drainage (HAND) map is developed. A Synthetic Rating Curve (SRC) was constructed based on the application of the Manning equation with reach-averaged geometries derived from the HAND map. With a time series analysis of measured discharges, inundation maps could be constructed linked to a return period.

The identified method was applicable in the Tirana region. Major benefits are the low computational requirements, easy applicable GIS operations and low data requirements, which make the method easily transferable to other regions. Constraints were found in the use of the coarse DEM with 25 meter resolution, which did not cover river geometries and local measures with high enough accuracy. This was solved by the manual inclusion of river geometries and verification of the developed inundation maps.

The Lana catchment is identified as the area most susceptible to flooding with an EAD of approximately one million Euro. One of the proposed measures, a multifunctional cross-section, proved to be most effective with a reduction of 65%. An urbanization scenario, in which the risk increased with 84%, demonstrated the need of the measures. Finally, the assessment revealed potential adverse effects of upstream measures on other areas and proved to add beneficial insights.

# Preface

In the beginning of my master water management, I participated in a project organized by the TU Delft | Delft Deltas, Infrastructures & Mobility Initiative (DIMI) in Japan. It was my first encounter with an interdisciplinary project and I enjoyed the experience very much. When I learned of another project, this time in Tirana, I was enthusiastic to participate again. In May 2018, students from TU Delft joined students from Tirana for an interdisciplinary workshop. The main topic was the development of flood risk reduction strategies and forms the starting point of this thesis.

The main objective of this additional thesis is to further investigate the results and designs that were developed in the workshop. In order to do so, a flood risk assessment is made to evaluate the effect of the proposed measures developed in the workshop.

I want to thank my supervisors Davide Wüthrich and Martine Rutten for their guidance and detailed feedback on my work. They have helped me a lot to guide my report and analyses. Furthermore I want to thank Fransje Hooimeijer and Mark Voorendt for organizing the project and their supervision in Tirana.

*S.P.C. Suijkens  
Delft, June 2021*

# Contents

<b>Abstract</b>	<b>i</b>
<b>List of Figures</b>	<b>v</b>
<b>List of Tables</b>	<b>vi</b>
<b>1 Introduction</b>	<b>1</b>
1.1 Background information . . . . .	1
1.2 Location information . . . . .	2
1.2.1 General information . . . . .	2
1.2.2 Topography . . . . .	2
1.2.3 Climate . . . . .	3
1.2.4 Flooding events . . . . .	4
1.3 Problem statement . . . . .	4
1.4 Objective . . . . .	5
1.4.1 Research questions . . . . .	5
1.5 Report structure. . . . .	5
<b>2 Literature study</b>	<b>6</b>
2.1 Flood types . . . . .	6
2.2 Flood risk definition . . . . .	6
2.3 Types of flood risk assessments . . . . .	7
2.4 Flood risk assessment methods . . . . .	8
2.5 Flood risk management . . . . .	10
<b>3 Materials and Method</b>	<b>11</b>
3.1 Data availability. . . . .	11
3.1.1 Discharge data . . . . .	11
3.1.2 Precipitation data . . . . .	12
3.1.3 Land use information . . . . .	12
3.1.4 Vulnerability information . . . . .	13
3.1.5 Topography of Tirana . . . . .	13
3.2 Method . . . . .	14
3.2.1 Main principles of method. . . . .	14
3.2.2 Hazard modelling . . . . .	15
3.2.3 Risk quantification. . . . .	16
3.2.4 Modelling measures . . . . .	16
3.3 Processing results of flood risk assessment . . . . .	16
<b>4 Data analysis</b>	<b>17</b>
4.1 Land use map development. . . . .	17
4.2 Time series analysis of discharges. . . . .	18
4.3 Discharge calculation tributaries . . . . .	19
4.4 Construction of HAND map. . . . .	20
4.5 Synthetic rating curve development. . . . .	21
4.6 Manning coefficient estimation. . . . .	23
4.7 Summary of hydraulic & risk parameters . . . . .	25
<b>5 Results</b>	<b>27</b>
5.1 Results of risk calculation . . . . .	27
5.1.1 Inundation maps . . . . .	27
5.1.2 Damage-probability curves . . . . .	30

---

- 5.2 Risk map . . . . . 30
- 5.3 Flood risk reduction. . . . . 32
  - 5.3.1 Waste removal and bank improvement . . . . . 32
  - 5.3.2 Modified cross-sectional area . . . . . 33
  - 5.3.3 Future urbanization projection . . . . . 33
- 6 Discussion and limitations 35**
- 6.1 Data sources . . . . . 35
- 6.2 Data processing review . . . . . 36
- 6.3 Risk assessment interpretation . . . . . 38
- 7 Conclusions 39**
- 8 Recommendations 41**
- Bibliography 42**

# List of Figures

1.1	Cross-section improvement . . . . .	2
1.2	Overview river basins Tirana region . . . . .	3
1.3	Climate statistics Tirana (BRIGRID, 2017) . . . . .	3
1.4	River site downstream of Tirana (BRIGRID, 2017) . . . . .	4
2.1	FN curve (Jonkman et al., 2017) . . . . .	6
2.2	Damage-probability curve (Messner et al., 2007) . . . . .	7
2.3	Flood inundation generation (Nootenboom, 2015) . . . . .	8
2.4	Effect of measures on FN curve (Jonkman et al., 2017) . . . . .	10
3.1	Maximum monthly discharge Gjola station 1951-1992 (Institute of Hydrometeorology, 1992) . . . . .	11
3.2	Depth-damage function Europe (Huizinga et al., 2017) . . . . .	13
3.3	FIAT schematization (Slager et al., 2017) . . . . .	14
3.4	Inundation mapping using HAND (Johnson et al., 2019) . . . . .	15
4.1	Land use map Tirana and surroundings . . . . .	17
4.2	Sub-catchments areas . . . . .	19
4.3	HAND map generation visualization . . . . .	21
4.4	HAND river geometry (Zheng et al., 2018) . . . . .	22
4.5	Division of Lana river, the arrows indicate the beginning and end of a section . . . . .	23
4.6	Flood mapping extent, modelled extent and HAND map used as source . . . . .	24
5.1	Accuracy of inundation map at Ishmi catchment . . . . .	28
5.2	Inundation maps per return period . . . . .	29
5.3	Damage-probability curve . . . . .	30
5.4	Risk map Ishmi basin . . . . .	31
5.5	Risk map Lana & Tirana catchment . . . . .	31
5.6	Risk comparison riverbed and bank improvement . . . . .	32
5.7	Risk comparison multifunctional cross-section . . . . .	33
5.8	Current land use Lana catchment . . . . .	34
5.9	Flood risk under influence urbanization . . . . .	34
6.1	HAND map generated with GRASS GIS & TauDEM in red . . . . .	36

# List of Tables

3.1	Peak precipitation flooding 2017 (Davies, 2017)	12
3.2	Precipitation Kamza station [mm]	12
3.3	Maximum damage values for Albania (Huizinga et al., 2017)	12
3.4	Open source topography datasets	13
3.5	Components for proposed method	14
4.1	CORINE Land Cover inventory	17
4.2	Gumbel parameters	18
4.3	Gjola station discharges per return period	18
4.4	Catchment area ratio	20
4.5	Discharges tributary per return period [ $m^3/s$ ]	20
4.6	Inundation stages tributary per return period [m]	23
4.7	Hydraulic & risk parameters per catchment	26
5.1	Damage and risk overview	30
5.2	Flood risk riverbed and bank improvement	32
5.3	Flood risk modified cross-sectional area	33
5.4	Flood risk overview future urbanization	34

# Introduction

## 1.1. Background information

Global economic losses due to flooding have increased over the last 50 years (Field et al., 2012). In 2012 19 billion dollar of losses were estimated (Ward et al., 2013; Munich Reinsurance Company, 2013). Flood risk is expected to increase in the next decades due to socio-economic development, subsidence and climate change (Ward et al., 2017). In many parts of the world flooding is the main cause of losses due to natural events (Kron, 2005) and by 2050 roughly 108 million people will live in urban areas susceptible to river flooding (PBL, 2021). In addition Kron (2005) describes floodplains as sites with easy accessibility for development, which has adverse effects in terms of flood risk. Under the influence of climate change, population increase and urbanization, governmental institutions face great challenges to address the increasing flood risk. Interdisciplinary urban planning can support mitigation of flood risk by identifying co-benefits of development. It is important to have insight in these factors in an early conceptual phase (Van Berchum et al., 2020).

Albania is susceptible to various natural hazards including earthquakes and flooding. In the last 20 years the flooding frequency has increased (Toto and Massabo, 2014). In December 2017, Albania faced the largest flooding event in history, in which almost 5000 households were affected (Davies, 2017). The capitol city, Tirana, was also affected by this flooding event and the city is facing several challenges in their approach to reduce flood risk. These challenges are related to a lack of planning and central governance on the topics of water management, transport and urban design, which led to several social, environmental and technical problems. In addition, with a GDP of 15,278 million USD, ranking 128th, financial means are often too little to address important issues. A field investigation in the flooded area in Tirana was performed under the Bridging the Gap for Innovation in Disaster resilience (BRIGAID) project. The main purpose of the field investigation was to obtain information from local residents on how they dealt with the flooding event and three areas in the Tirana region were identified for further investigation in the form of a case study.

The three areas from the BRIGAID project formed the basis for an interdisciplinary workshop in May 2018, in which a group of students from five disciplines from the TU Delft visited Tirana. Together with students from three universities in Tirana an interdisciplinary design for the three areas in the city was made. One of the areas that was investigated is the urban area along the Lana river, which include the city centre and a suburban area. The hydraulic capacity of the river is affected by urban waste and several reaches where the cross-section is in a bad maintained state. In addition the area has urbanized fast in the recent years (BRIGAID, 2017), leading to an increase in flood risk. The main results from the workshop included (preventive) measures to reduce urban waste and a multifunctional cross-section (figure 1.1), with higher hydraulic capacity at peak flow conditions, linked to the transport system. The outcome from the workshop forms the starting point for this research and will be further investigated in terms of flood risk reduction.

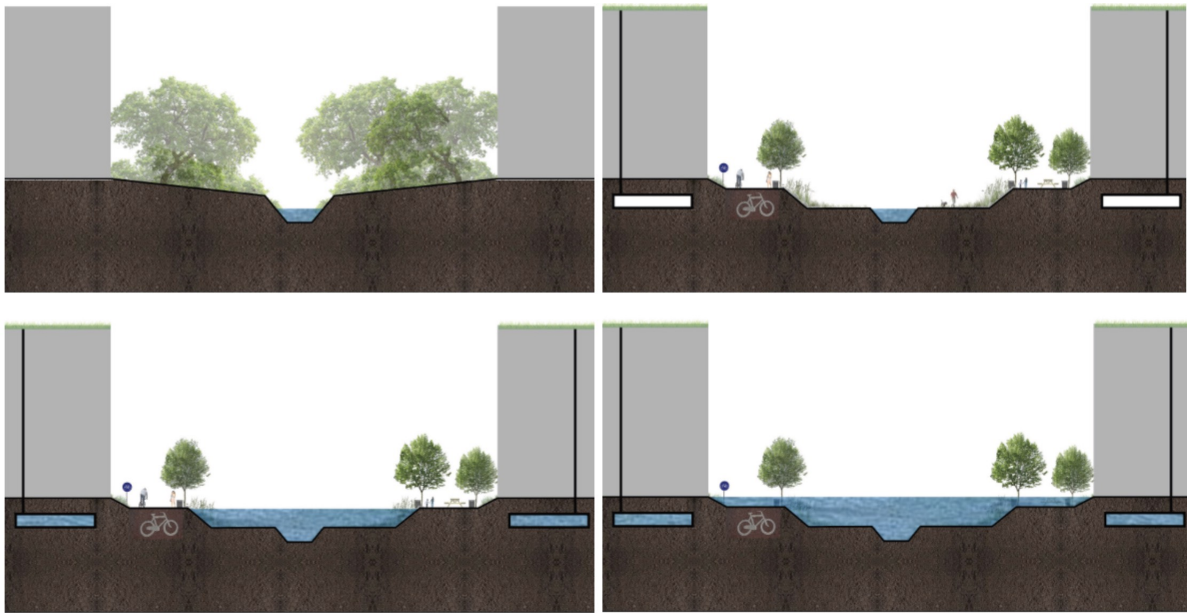


Figure 1.1: Cross-section improvement

## 1.2. Location information

### 1.2.1. General information

Albania is located in south-eastern Europe and borders the Adriatic and Ionian sea. The total area is 28,748 km<sup>2</sup> and Albania has around 3 million inhabitants (CIA, 2021), with Tirana as major city with 500,000 inhabitants. In 1990 reforms were made by the communist government and the republic of Albania was founded. The political history has an effect on the availability of data, as no continuously state archive is present (Toto and Massabo, 2014). After the fall of the communist regime massive migration out of Albania took place with in addition internal migration towards the cities of Durrës and Tirana. Although the total urban population is relatively low with 52%, the annual rate of change is high with 2.3% (Toto and Massabo, 2014). Between 1990 and 1994 the physical growth of the city was four times more than in the period 1945-1985, leading to unmanaged development (Aliaj, 2002). As of 2019 the GDP per capita was \$5,353.2 (Worldbank, 2021).

### 1.2.2. Topography

Tirana is located in the Ishmi basin, with a size of 705km<sup>2</sup>. The Ishmi river consist of five main tributaries: Lana river, Tirana river, Zeze river, and the Terkuzi river (BRIGAD, 2017). Their origin is in the mountainous area to the north-east of Tirana and are related to the flooding events in Tirana. A smaller tributary of the Ishmi river is the Limuthi and it has its origin in the mountainous area west of Tirana. The most dense urban area and city centre of Tirana is enclosed by the Tirana and Lana river. The rivers have a relatively high slope before they reach the city. Towards the merging point into the Ishmi river the slope becomes relatively low.

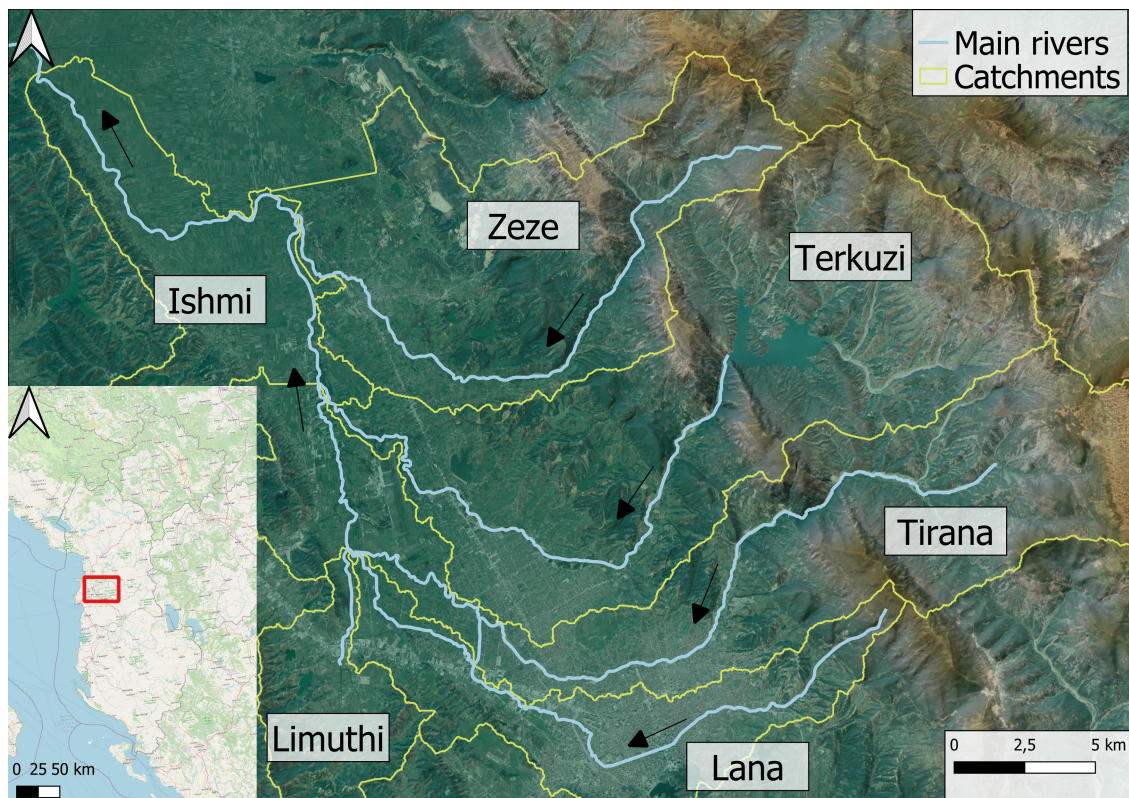


Figure 1.2: Overview river basins Tirana region

### 1.2.3. Climate

Tirana lies within the Mediterranean climatic zone. The annual average temperature is 15.1°C. The driest month of the year is July and most precipitation occurs in the winter months. Around 80% of annual rain is measured between October-March, with the maximum in November at 174mm (BRIGAID, 2017). Graphs can be seen in figure 1.3.

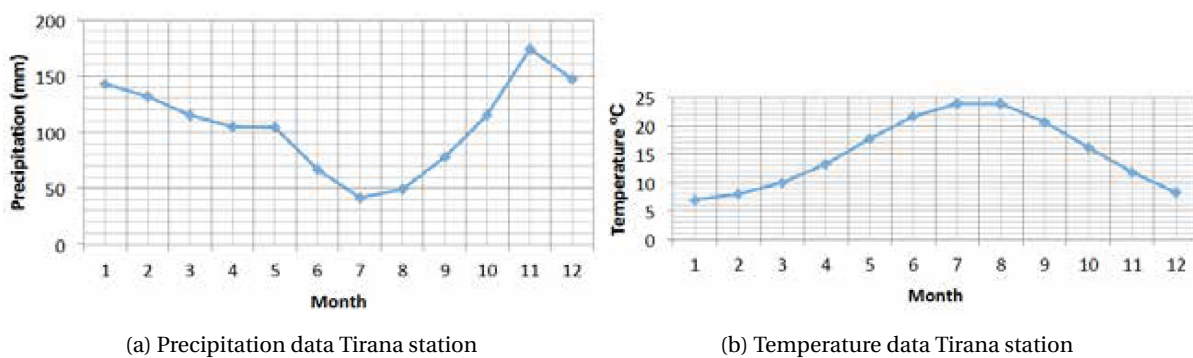


Figure 1.3: Climate statistics Tirana (BRIGAID, 2017)

### 1.2.4. Flooding events

The historical floods and damages have been investigated by Toto and Massabo (2014). When the temporal behaviour of floods is considered an increase in the number of events is described by Toto and Massabo (2014) between 1946 to 2013. On average 23 flooding events occurred every year and at least 54% of the regions in Albania have experienced a flood. The average mortality rate in the last 20 years is 0.05 per event. The average expected losses have been estimated at 3.2 million dollar per year, with a peak of 35.2 million dollar in 2010. In terms of extent the agricultural sector is affected the most by flooding events in Albania. In 2010 almost 10,000 houses were affected by flooding. A considerable problem is the existence of informal housing, often built in close proximity to the river. In addition in the 2017 flood near Tirana severe indirect damages occurred. The main road between Tirana and Durres was closed and this induced economic losses. Several businesses along the road were affected through production losses.

For Tirana the main types of flooding are river flooding and flash floods, both induced by high volumes of precipitation. For Tirana snow melt in spring has not been an important factor. Consecutive days with moderate-intense precipitation can lead to riverbank overflow. In winter these flooding events can last for weeks. In addition urban drainage problems are increasing, due to clogging of the drainage system. High intensity rain events can lead to flash floods in the area. Due to the close proximity to mountainous areas the response time for flooding is relatively low. Travel times through the main river networks are estimated at 8-10 hours for flash floods (Selenica et al., 2011). The area is protected by earthen levees and erosion problems in the catchment often endanger the flood protection. Furthermore river obstruction by sediment and waste can lead to local overflow, see figure 1.4.



Figure 1.4: River site downstream of Tirana (BRIGRID, 2017)

## 1.3. Problem statement

Global flood risk is increasing and is expected to be the main cause for economic losses. In Albania and the city of Tirana flooding events and damages have increased over the past 20 years. A lack of general overview and interdisciplinary approaches could cause an increased vulnerability and thus risk. Proper identification of high risk areas and the influence of future development is of importance to create awareness at governmental level and residential user level.

As in many developing countries, data for flood risk assessments in urban areas is very scarce in Albania. Global flood risk assessment methods using open source data are often not applicable due to resolution and quality limitations. The constraints to easily identify urban flood risk imposes a problem to integrate flood risk measures in urban designs during early developing stages.

## **1.4. Objective**

The first objective of this thesis is to develop a method usable in urban areas with poor or scarce data to quantify and advise on flood risk reduction measures. The method should support decision making and conceptual designs during interdisciplinary cooperation. Secondly the proposed method should be applied for the city of Tirana and surroundings and thereby quantify and connect the flood risk reduction measures as proposed in the student workshop.

### **1.4.1. Research questions**

- What method can be used to assess flood risk in urban areas with scarce data?
- What are the minimum requirements in terms of data quality and accuracy to assess urban flood risk?
- Which areas in Tirana are susceptible to flooding?
- What is the effect of the proposed measures in the workshop in terms of flood risk reduction?

## **1.5. Report structure**

In chapter 2 the general theory of flood risk assessments is discussed, as well as the current assessments and methods. Chapter 3 focusses on the materials used for the risk calculation and in section 3.2 the general outline of the method and approach is explained. Chapter 4 gives in detail explanation of the inputs and pre-processing of the assessment method. In chapter 5 first the produced inundation maps are presented, then the risk assessment is presented and finally the risk reduction measures are quantified. The results are discussed in chapter 6.

# 2

## Literature study

### 2.1. Flood types

By the Cambridge dictionary a flood is defined as "a large amount of water covering an area that is usually dry." Three main types of flooding and several special cases can be described (Jonkman, 2005; Kron, 2005):

- Coastal floods (storm surges): occurrence along coastline and big lakes. Driven by wind and low atmospheric pressure, water levels are set-up along the coast. Coastal flooding can cause the highest losses in terms of lives and property.
- River floods: flooding of the river outside the normal boundaries. Can be caused by high precipitation and/or snow melt. Usually river flooding can be predicted, with the exception of breaches of river dikes or dams.
- Flash floods: flooding with a sudden onset and local character, usually caused by high intensity precipitation. Despite the local character flash floods have a high potential for damage and loss of life, mainly because of the low predictability.
- Special cases: water logging, tsunamis.

### 2.2. Flood risk definition

Different definitions of risk can be defined. In general risk is seen as the product between the probability of an (extreme) event and the consequences of that event. (Jonkman et al., 2017). The focus and indices of these consequences can differ. When loss of life is considered the risk can be displayed using a FN curve (see figure 2.1), which can be transferred to a FD curve when damage is considered.

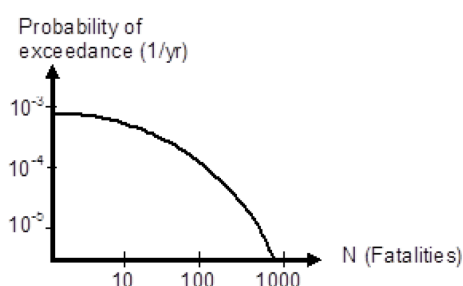


Figure 2.1: FN curve (Jonkman et al., 2017)

The quantification of risk in a monetary value can be described by the Expected Annual Damage (EAD) (Verkade and Werner, 2011):

$$\int_0^1 D(P) dP \quad (2.1)$$

In which  $P$  is the annual probability of exceeding a flood level and  $D(P)$  is direct damage caused by that flooding event. Risk is thereby seen as the integral of the probabilities of non exceedance (Winsemius et al., 2013). The results of equation 2.1 can be plotted in a damage-probability curve, in which the total area under the curve represents EAD. In addition the effects of implementing flood protection standards can be visualized, see figure 2.2.

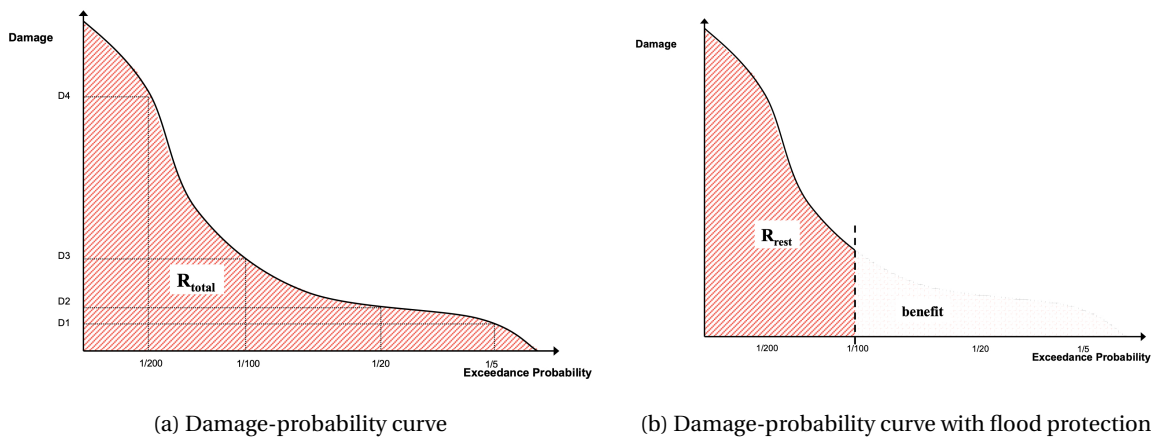


Figure 2.2: Damage-probability curve (Messner et al., 2007)

### 2.3. Types of flood risk assessments

A damage based approach is described by Merz et al. (2010). It is stated that flood risk assessments often focus more on the modelling of the hazard. As flood risk management becomes the dominant factor in flood control policies in Europe, a better balance between hazard and damage assessment is opted. Merz et al. (2010) claims that in the current situation a mismatch occurs between the quality of damage data and models compared to its high relevance. An example is the simplification of complex damage mechanisms by depth-damage curves. Merz et al. (2010) also describes how the effect of flooding can be divided into several categories. First a difference between direct and indirect damage is distinguished. Where direct damage is caused by direct contact of assets with flood water. Indirect damage is related to damage outside the flood prone area or after the flooding event. Furthermore tangible and intangible damage is explained. Tangible damage is possible to express in a monetary value whereas intangible damage is usually difficult to describe in a monetary value.

Jonkman (2007) developed a general method to estimate loss of life and quantify the risk. Later he applied this methodology to flooding events. For loss of life due to flooding the estimate can be given by three factors: flood characteristics, exposed population & evacuation and mortality estimate among the exposed population. The method is applicable for low-lying areas protected by flood defences.

Tapsell et al. (2002) describes the discrepancy between most used models and the possibility to estimate intangible effects on flooding. Tapsell et al. (2002) attempt to develop models that predict the social impacts of flood assessment, which gives the possibility to find a better balance between damage based and societal based modelling. To assist in finding this balance a "Social Flood Vulnerability Index (SFVI)" is developed.

An important aspect of damage based flood risk assessments is quantification of the uncertainty. The uncertainties and errors in the damage estimate can affect decision-making (Wagenaar et al., 2016). Wagenaar et al. (2016) demonstrated uncertainties in damage estimation of the order 2-5. He introduced a method to quantify the uncertainty for river flooding. A distinction is made between epistemic and aleatory uncertainty. Aleatory uncertainty is caused by using average data for damage estimation. Especially for small flooding events aleatory uncertainty is high, while for larger events the individual difference are cancelled out more.

Epistemic uncertainty is related to "the lack of understanding a system" (Wagenaar et al., 2016). This uncertainty is introduced when data from an event is transferred to other areas or events. With larger flooding events this uncertainty does not decrease and is therefore the most important uncertainty. The application of damage-functions is susceptible to epistemic uncertainty.

## 2.4. Flood risk assessment methods

Several methods can be used to compute flood risk. An important factor is data availability and data quality. A difference between open source data and commercial data can be distinguished, the latter providing often better local quality. To generate methods with easy applicability the use of open source data is highly preferable. This high applicability of methods is especially of importance for flood risk assessments in developing countries and/or areas with poor data. Robust methods that use open source data are available on a global scale. However, on an urban scale flood risk assessments often rely on local commercially available data and intensive hydro-dynamic modelling. The use of open source data on an urban scale is still challenging because of the quality and spatial resolution. An example of methods that use open source data or operate with scarce data is further elaborated upon in this section.

A framework to strategically describe global flood risk by river flooding is described by Winsemius et al. (2013). The framework is called "GLObal Flood Risk with IMAGE Scenarios" (GLOFRIS) (Winsemius et al., 2013). GLOFRIS combines hazard, exposure and vulnerability. To derive hazard the global hydrological model PCR-GLOBWB (Van Beek and Bierkens, 2008) is used in combination with DynRout. The output of PCR-GLOBWB is 0.5 x 0.5 degrees (50km) and downscaled to 30 arc seconds (1km). The main approach to reach inundation levels is to impose the water volume above a river pixel. The water volume that is in excess of the bank-full capacity is distributed over the surroundings using a Digital Elevation Model (DEM). The result is an inundation map on a DEM with 1km resolution for different return periods, see figure 2.3. The method is less applicable for small scale pluvial flooding. Winsemius et al. (2013) further used a population and land-use based method to indicate exposure and vulnerability. Ward et al. (2013) further extended the method to a global scale with more return periods taken into consideration.

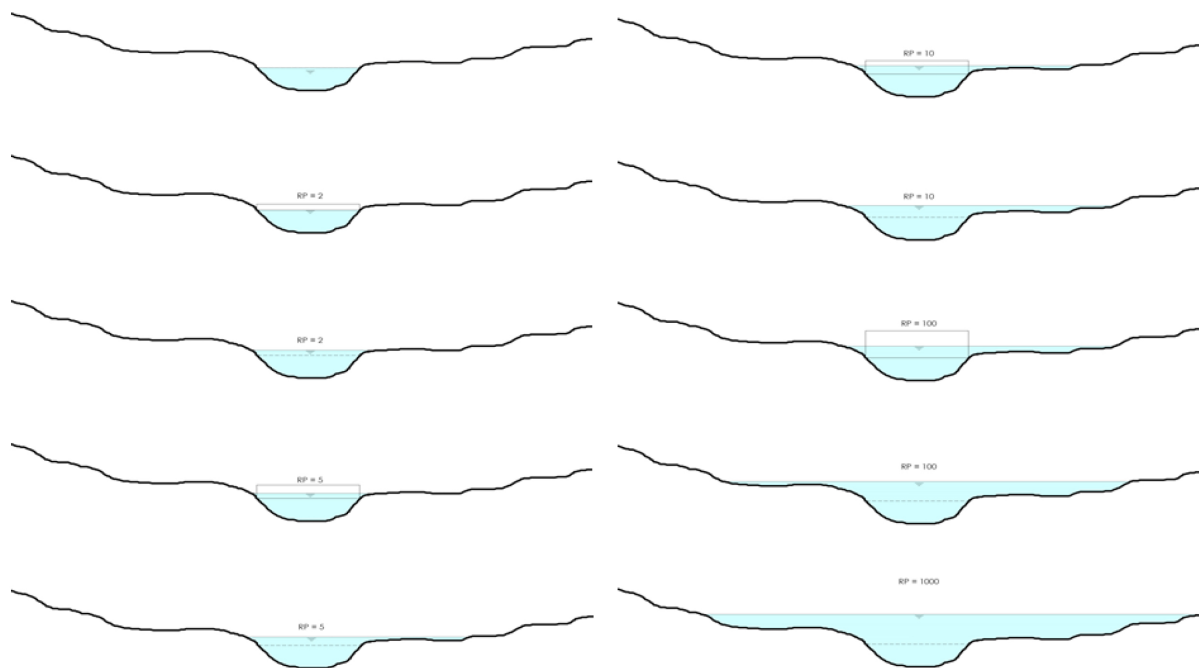


Figure 2.3: Flood inundation generation (Nootenboom, 2015)

Nootenboom (2015) used the hazard generation method of Winsemius et al. (2013) to derive a global flood risk index for urbanized areas near rivers. Global Rural-Urban Mapping Project (GRUMP) urban extent was used to define city boundaries and combined with Moderate Resolution Imaging Spectroradiometer (MODIS) data. This resulted in a land use class specified in urban and peri-urban. Different coverage and maximum damage values were used and only one damage function. For Europe a multiple land use assessment was performed. More detailed land use information is available by CORINE Land Cover (CLC) inventory. Furthermore detailed depth-damage functions per continent and maximum damage values per country are derived (Huizinga, 2007; Huizinga et al., 2017). When the single land use and multiple land use method are compared a high correlation of 0.97 is observed for Europe. However, it is shown that a large overestimation of flood risk is made when using one land use class. Furthermore the effect of climate change and socio-economic development is assessed showing areas with low protection standards are most vulnerable to climate change.

In an attempt to extend the multiple land use method of Nootenboom (2015) to a global scale, research was done in land use information from OpenStreetMap (OSM) (Suijkens, 2015; Kusters, 2015; Van der Veer, 2015) Continent specific depth-damage functions by Huizinga (2007) were used. For Australian cities a coverage up to 62% was reached with OSM. The flood risk assessment showed a correlation of 0.99 with Nootenboom (2015) and a similar decrease in actual flood risk when using multiple land use classes. The derived land use maps from OSM and method were later successfully used by Verschuur (2016) in a case study for Bangkok.

Van Berchum et al. (2020) developed the Flood Risk Reduction Evaluation and Screening (FLORES) model, which aims to provide flood risk in a conceptual phase of design. It thereby stresses the computational constraints of traditional flood simulation software, in which it is time consuming to model several flood risk reducing strategies. In addition this simulation software often needs high quality data as an input (Van Berchum et al., 2020). The FLORES model is intended to be used with minimal detailed local data. A case study for Beira, Mozambique is performed. The source code of the model is written in a manner that transferability to other flood prone cities is possible. For urban flooding an urban inundation model and drainage system model are combined. Rainfall and storm surges are taken into account. The damages due to flooding are calculated using the expected damage, the number of people affected and the cost of repair. FLORES is able to evaluate the influence of different combinations of flood risk reduction strategies. The model uses the Exploratory Modelling and Analysis (EMA) workbench to visualize and support decision making (Van Berchum et al., 2020). Although many inputs of the FLORES model are globally available, the DEM that is used was locally obtained and has a resolution of 2 meter. It is expected that the model will also operate with a resolution of 12 meter. This would indicate that the use of ALOS-PALSAR data is possible, with resolutions up to 12.5m. However, currently there remain still large data gaps in the ALOS-PALSAR dataset. Globally available DEM data with 30m resolution has not been evaluated yet within the FLORES model.

A method to derive flood inundation maps, without the use of (complex) hydro-dynamic modelling, is described by Johnson et al. (2019). A terrain based approach, using a Height Above Nearest Drainage (HAND) map, is developed to map inundation for several catchments in the United States. The main inputs for the method are land elevation data, stream flow inputs and discharge-height relationships. By imposing a certain discharge on a stream flow, the accompanying water level is imposed on the surrounding area. The method proved to be applicable as a "high-level guidance tool" (Johnson et al., 2019). For areas without stage-discharge relationships the development of a synthetic rating curve is described by Zheng et al. (2018). The method of Johnson et al. (2019) and Zheng et al. (2018) is used in this research and further explained in section 3.2.2.

## 2.5. Flood risk management

Reasoned from the main definition of flood risk, reduction can be reached through the reduction of the probability of flooding or reducing the negative consequences (Jonkman et al., 2017). This approach is visualized in figure 2.4.

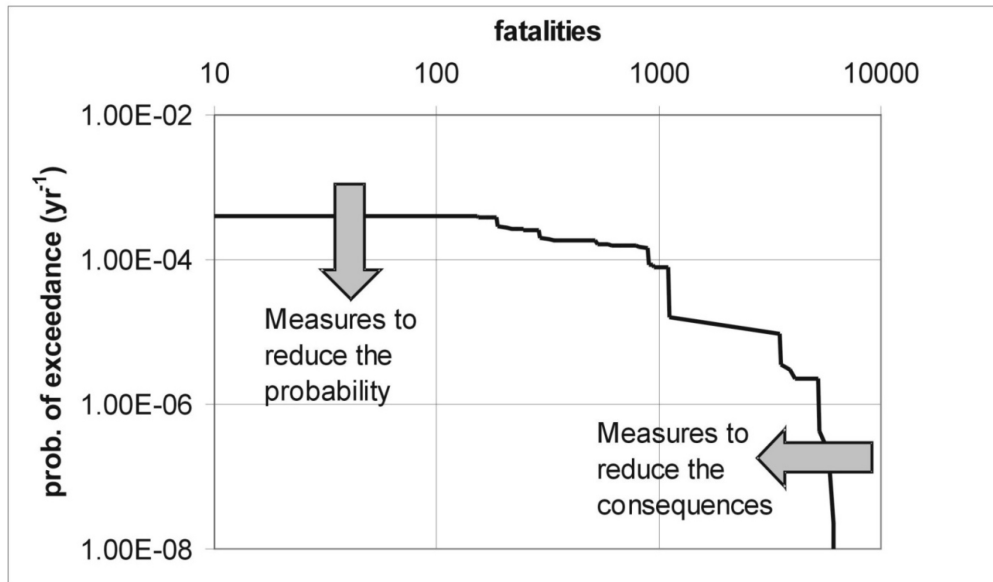


Figure 2.4: Effect of measures on FN curve (Jonkman et al., 2017)

A distinction can be made between structural and non-structural measures. Well known structural measures are dikes, levees and dams which reduce the probability of flooding. In general these engineering-based measures will be costly to implement (Van der Pol et al., 2015). An important non-structural measure is flood warning through flood forecasting and is named the most effective measure (Verkade and Werner, 2011). In addition urban planning based on the flooding probability could reduce the exposure and/or vulnerability.

An important aspect of flood risk management is the cost effectiveness of measures and strategies. The most direct way to express the effectiveness is through the benefit/cost ratio which should be greater than one (Jonkman et al., 2017). To deal with the risk reduction benefits that span over a longer period of time, the Nett Present Value (NPV) can be used. It is described by equation 2.2 (Jonkman et al., 2017).

$$NPV = \sum_{i=1}^T \frac{C_i}{(1+r)^i} \quad (2.2)$$

With:

- $r$  is the discount rate
- $C_i$  is the cost in year  $i$  [€]
- $T$  is the reference period in years

A model to evaluate the different combination of risk reduction strategies is presented by Van Berchum et al. (2019) and is called Multiple Lines of Defence Optimization System (MODOS)-model. It is implemented in the FLORES model as mentioned in section 2.4. By using the model it is possible to take the interdependency of reduction measures into account.

## Materials and Method

### 3.1. Data availability

In this section the available data is presented.

#### 3.1.1. Discharge data

As mentioned in section 1.2.1 continuous datasets are difficult to obtain. Data that is available is usually stored in local archives and has not been digitalized yet (Toto and Massabo, 2014). Lushaj et al. (2011) mentions that the Department of Water Economy and Renewable Energy (IGEWE) is responsible for all water resources measurements. Currently 105 manual stations are in place, from which measurements are sent monthly by regular mail to IGEWE. All rating curves are outdated. The World Bank funded 20 automatic stations and Acoustic Doppler Current Profilers (ACDP) were acquired (Lushaj et al., 2011). However, as of today this discharge data has not been made available.

For the Ishmi river monthly discharge measurement for the period 1951-1992 have been obtained from the Institute of Hydrometeorology. The measurement location is positioned at the Gjola bridge, downstream of the Lana, Tirana, Limuthi and Terkuza river tributary. In figure 3.1 a histogram of the dataset is presented. This dataset is used to derive discharges for the upstream tributaries based on the catchment areas.

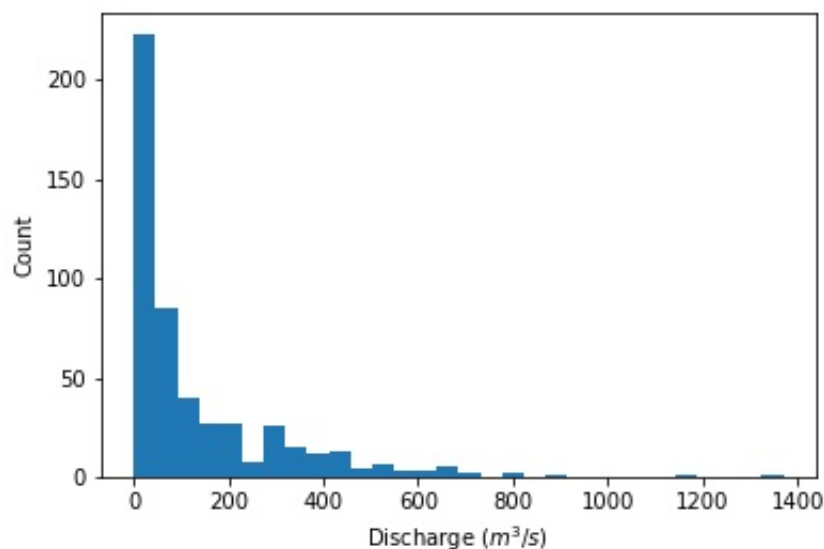


Figure 3.1: Maximum monthly discharge Gjola station 1951-1992 (Institute of Hydrometeorology, 1992)

### 3.1.2. Precipitation data

For the flooding event of 2017, 24h precipitation values are described by (Davies, 2017) and listed in table 3.1. In addition Bogdani and Selenica (1997) describes the maximum 24 hour precipitation as 300-400mm in the North and as 200-300mm in the Southern mountainous region of Albania.

Table 3.1: Peak precipitation flooding 2017 (Davies, 2017)

Region	Precipitation (mm/24h)
Shkodra	63
Kukes	126
Tirana-la Praka	121
Gjirokastra	146
Peshkopi	61

Precipitation data for the Kamza station, located 20km outside of the city centre of Tirana is listed in table 3.2.

Table 3.2: Precipitation Kamza station [mm]

T [1/yr] ->	100	50	20	10	5	2
10 min	24	22	20	18	15	12
20 min	41	39	33	29	25	18
30 min	57	51	43	37	31	22
60 min	76	68	58	50	41	29
120 min	83	75	65	57	48	35
360 min	106	96	83	74	63	48
720 min	144	130	110	96	80	57
1440 min	192	174	148	128	108	76

### 3.1.3. Land use information

As described in section 2.4, OpenStreetMap and CORINE Land Cover (CLC) inventory were used in previous assessments. For Tirana the coverage with OpenStreetMap is estimated at 60%. The data is available in vector format and can be rasterized at the desired resolution. Albania is covered in the CLC inventory with a resolution of 100x100m. In the dataset 48 land use classes are distinguished. In previous assessments five land use classes were used, based on the availability of damage values by Huizinga et al. (2017). In this research four land use classes will be used. The 48 land use classes can be converted to these four classes, which are: residential, commercial, agricultural and infrastructure land use. Maximum damage values are given on a country level. Furthermore these are listed in three categories: building based, land-use based and object based. The land use based values are listed in table 3.3.

Table 3.3: Maximum damage values for Albania (Huizinga et al., 2017)

Land use class	Maximum damage value
Residential	65 €/m <sup>2</sup>
Commercial	143 €/m <sup>2</sup>
Agriculture	1417 €/ha
Infrastructure	2.40 €/m <sup>2</sup>

### 3.1.4. Vulnerability information

The most comprehensive dataset for vulnerability is given by Huizinga et al. (2017). Depth-damage functions are given per continent and land use class, see figure 3.2 for the European depth-damage functions that are used in this research.

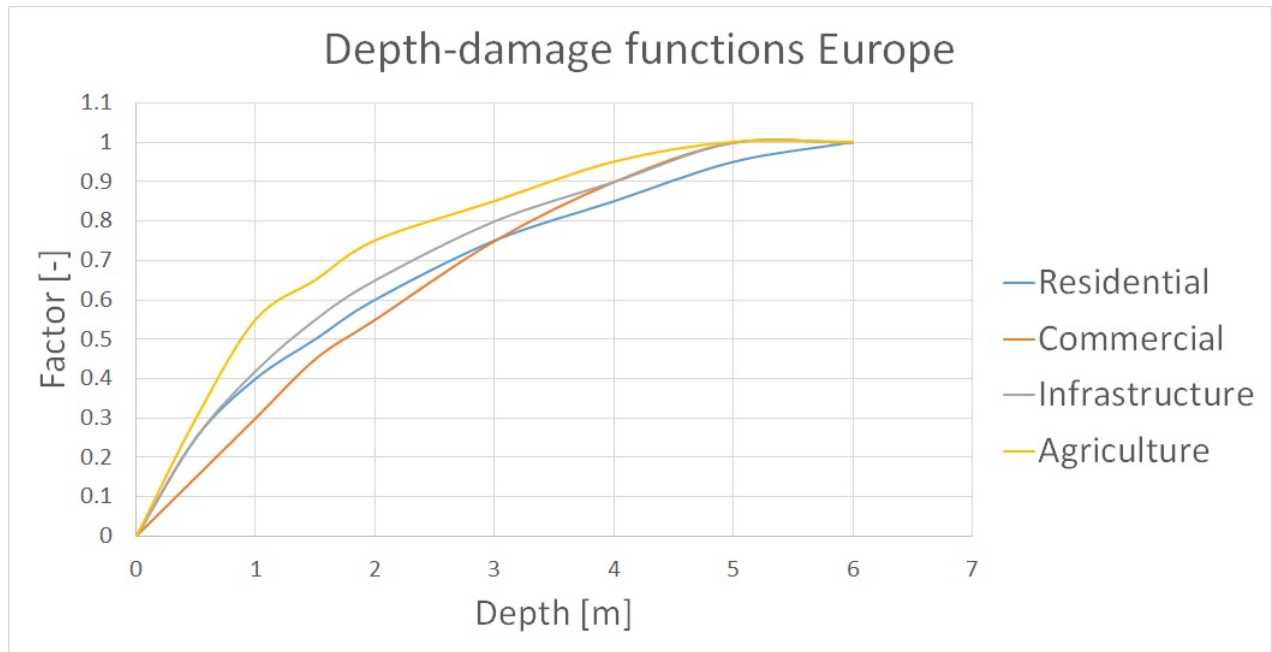


Figure 3.2: Depth-damage function Europe (Huizinga et al., 2017)

### 3.1.5. Topography of Tirana

To describe the topography (of the Tirana area) several open source datasets are investigated and listed in table 3.4.

Table 3.4: Open source topography datasets

Dataset	Information type	Resolution	Provider
USGS DEM	Land elevation (m)	30 x 30m	USGS Earth explorer
EU-DEM	Land elevation (m)	25 x 25m	Copernicus
EU-Hydro	River network	1:30.000	Copernicus
EU-Hydro	Drainage network	1:50.000	Copernicus
ALOS-PALSAR	Land elevation (m)	12.5 x 12.5m	<b>No coverage</b>

The most accurate open source dataset for land elevation, ALOS-PALSAR, has no coverage for Albania. The river network from EU-Hydro is derived with 20m resolution imagery and the drainage network is derived from the 25m DEM. The rivers considered in this research have a Strahler order of 1 to 4.

## 3.2. Method

In this section, based on the available data, a method is proposed to assess flood risk on an urban scale with open source data, applied on the city of Tirana and its surroundings.

### 3.2.1. Main principles of method

A damaged based flood risk assessment following the principles of (Winsemius et al., 2013) is proposed, using the product of *hazard*, *vulnerability* and *exposure* as main components. The first step is to transfer the selected data into compatible formats, making multiplication possible.

Table 3.5: Components for proposed method

Component	Type
Hazard	Inundation depth (m)
Vulnerability	Depth-damage function (factor)
Exposure	Land use classes (m <sup>2</sup> )

With the use of GIS all data can be pre-processed into raster files with the same extent and format. To simplify and organize the damage calculation, the Flood Impact Assessment Tool (FIAT) from Deltares can be used. It is a open source Python based tool that combines the required data into a damage map. Additionally, when relationship between the inundation depth and the return period can be identified, a risk profile can be determined expressed in expected annual damage. A visual overview of the FIAT work flow is presented in figure 3.3.

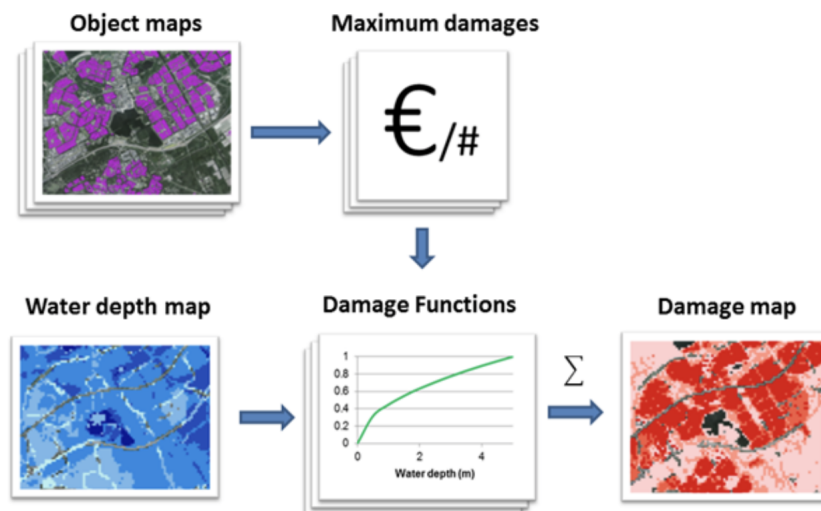


Figure 3.3: FIAT schematization (Slager et al., 2017)

The Tirana area can be divided into multiple sub-catchments which makes it possible to estimate damages per area and identify areas most susceptible to flooding, thereby making it possible to model local measures and quantify the effect.

### 3.2.2. Hazard modelling

As seen in section 2.4, hydrodynamic models require accurate local data and are computationally heavy to operate. To make the method transferable and possible to operate without this data requirements, a terrain based approach is used as described by Johnson et al. (2019) and Zheng et al. (2018).

The precise method to derive flood inundation depth is explained by Johnson et al. (2019). It requires a DEM and spatial representation of the river network, which are both available for the Tirana region. The work flow of the method is visualized in figure 3.4.

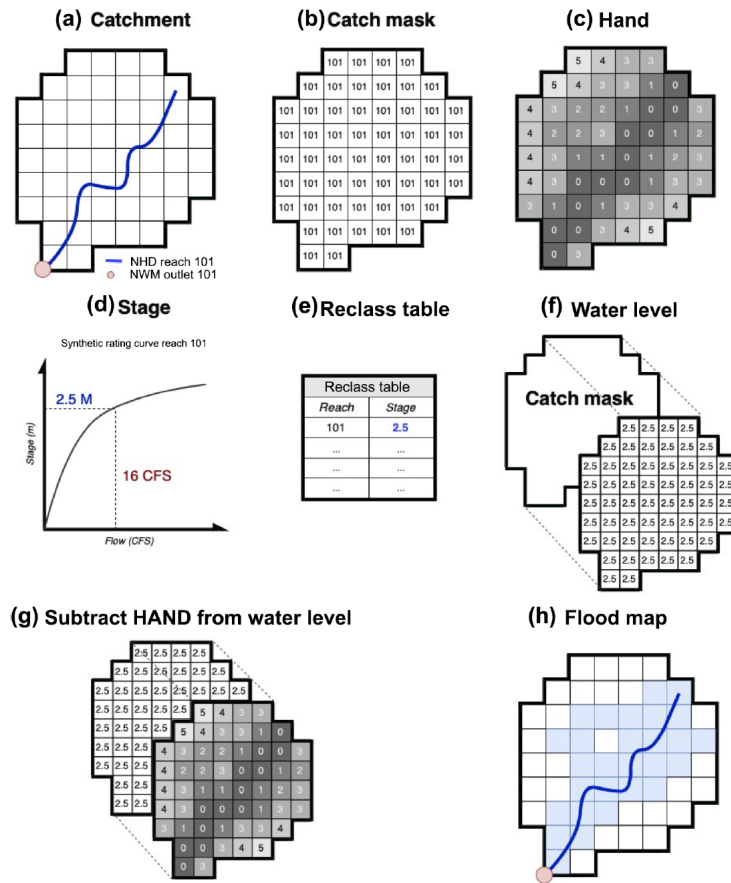


Figure 3.4: Inundation mapping using HAND (Johnson et al., 2019)

In the first step a river segment and the corresponding catchment is defined. For each catchment a Height Above Nearest Drainage (HAND) map is generated. This map indicates for each raster pixel the vertical distance to the nearest stream. Then the stage-discharge relationship for the river segment is used to connect the discharge to a stage of the river. A mask for each stage of the river is created and subtracted by the HAND map. If a raster cell contains a positive value it indicates inundation for that cell.

The synthetic rating curve (SRC) can be constructed based on geometries derived from the HAND map, as described by Zheng et al. (2018). In this method a stage for the river is assumed and the steps as described in figure 3.4 are used. For each stage the number of wet cells and their values are determined to calculate the flood volume. Making use of the flood volume a reach-average cross-sectional area and reach-average hydraulic radius are derived. These parameters are used in the Manning equation resulting in a discharge corresponding to a stage of the river. By repeating this procedure for incrementally increasing stages a SRC is formed.

### **3.2.3. Risk quantification**

By making use of the Flood Impact Assessment Tool a damage value will be connected to a return period as shown in figure 2.2. Then the tool is able to derive the expected annual damage to quantify the risk. To obtain the return periods corresponding to a flooding event a time series analysis of the discharge data will be performed in section 4.2. Within the tool it is also possible to specify the current flood protection level, expressed as a return period. Corresponding to figure 2.2 a part of the damage-probability curve will be neglected in the risk summation.

### **3.2.4. Modelling measures**

After identification of areas most vulnerable for flooding, local measures can be investigated. Based on the type of measure either the hazard, vulnerability or exposure input can be adjusted for a specific area.

The effect and applicability of measures can be quantified based on the risk parameter used as explained in section 3.2.3. With the EAD, a cost benefit analysis can be performed using the cost/benefit ratio and equation 2.2. Within the scope of this thesis a quantification of the risk reduction will be made, without a cost/benefit study. The design of the workshop will be used for the Lana catchment. Thereby for two measures and one future scenario the risk will be calculated.

## **3.3. Processing results of flood risk assessment**

The calculated damages, risk and effects of modelled measures will be presented in tables and visualized using Qgis. Furthermore, through risk maps the specific areas in the Tirana region most susceptible for flooding can be identified. Risk maps generated with modelled measures can be compared to risk maps without measures in place to visualize the effect.

# 4

## Data analysis

### 4.1. Land use map development

The land use classes of the CLC Cover dataset are studied for the research area. Each land use class is assigned a specific raster cell value. By making use of the raster calculator in Qgis land use classes of interest are extracted and combined into 4 land use classes. No specific distinction between industrial and commercial areas can be derived for Tirana, therefore they are combined into the commercial land use. In table 4.1 an overview is given and the corresponding land use map is presented in figure 4.1.

Table 4.1: CORINE Land Cover inventory

Class	Description	Cell value	Allocated land use
111	Continuous urban fabric	1	Residential
112	Discontinuous urban fabric	2	Residential
121	Industrial or commercial units	3	Commercial
122	Road and rail network	2	Infrastructure
123	Airports	6	Infrastructure
211 - 244	Agricultural areas	12-22	Agricultural

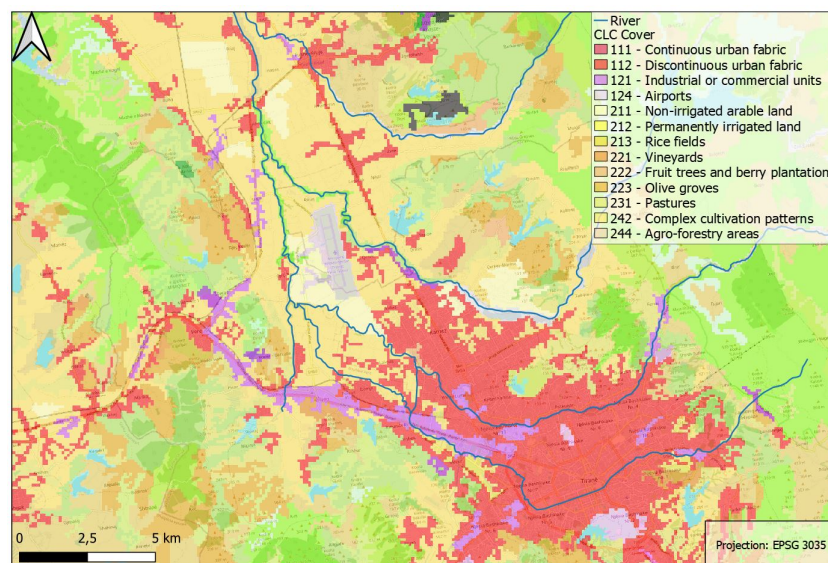


Figure 4.1: Land use map Tirana and surroundings

## 4.2. Time series analysis of discharges

For each year of the data series presented in section 3.1.1, the maximum value is noted. The Gumbel distribution, described by equation 4.1, is used to analyse these annual maxima.

$$F(x) = \exp(-\exp(\frac{x - \mu_0}{\beta})) \quad (4.1)$$

with:

$$\mu_0 = -\beta * \ln(\frac{1}{n} \sum_{i=1}^n \exp(\frac{-\mu_i}{\beta})) \quad (4.2)$$

$$\beta = \frac{1}{n} \sum_{i=1}^n (\mu_i) - \frac{\sum_{i=1}^n (\mu_i) * \exp(\frac{-\mu_i}{\beta})}{\sum_{i=1}^n \exp(\frac{-\mu_i}{\beta})} \quad (4.3)$$

With equation 4.4 and 4.5 a first estimate for  $\mu_0$  and  $\beta$  is derived. Subsequently these equations are solved iteratively. An overview of the parameters is given in table 4.2.

$$\beta = \frac{\sigma\sqrt{6}}{\pi} \quad (4.4)$$

$$\mu_0 = \mu - 0.5772\beta \quad (4.5)$$

Table 4.2: Gumbel parameters

Parameter	Value [ $m^3/s$ ]
mean	530.05
standard deviation	233.95
$\mu$ initial	424.76
$\beta$ initial	182.41
$\mu$ iterative	429.60
$\beta$ iterative	172.55

When equation 4.6 is solved for T the corresponding discharge for several return periods can be calculated. This results in the discharges for the Ishmi river at the Gjola station as presented in table 4.3.

$$x = \beta \ln(-\ln(1 - \frac{1}{T} + \mu_0)) \quad (4.6)$$

Table 4.3: Gjola station discharges per return period

Return period [1/T]	Discharge ( $m^3/s$ )
5	688
10	818
25	981
50	1103
100	1223
250	1381

### 4.3. Discharge calculation tributaries

No discharge data for the Lana, Tirana, Limuthi and Terkuzi river is available. Therefore these discharges are derived from the discharges at the Gjola station at the Ishmi river. It is thereby assumed that the discharge of the Ishmi river at the measurement location consists of the sum of its tributaries. The area of each tributary catchment is calculated and the ratio is determined. This ratio is then used to derive the discharge per tributary in the absence of more precise data. It is thereby assumed that precipitation is distributed homogeneous over the entire catchment area. The Zeze river joins the Ishmi river further downstream the measurement location, therefore no discharges for the Zeze river could be derived. The Zeze catchment is thus excluded from further flood risk assessments. In figure 4.2 and table 4.4 the areas of the sub-catchments are indicated that are used to achieve the discharges in table 4.5.

Since peak flow conditions are being evaluated, fast flow processes are of importance to include. The catchment areas with a large hard surface area will have a more dominant contribution to the discharges in the Ishmi river during peak flow. Therefore for each catchment the distribution of hard and soft land cover is determined. A run-off coefficient for hard land cover of 0.8 is estimated and for soft surfaces 0.3. By including these surface characteristics the "effective contributing area" to the peak flow is calculated. The discharge for each tributary is scaled making use of this parameter. An overview of this calculation is presented in table 4.4. It can be clearly seen that the Lana river has a larger share of the discharges with scaling. This is consistent with the presence of dense urban areas in this catchment. Furthermore the calculated discharges per tributary are presented in table 4.5 for each return period.

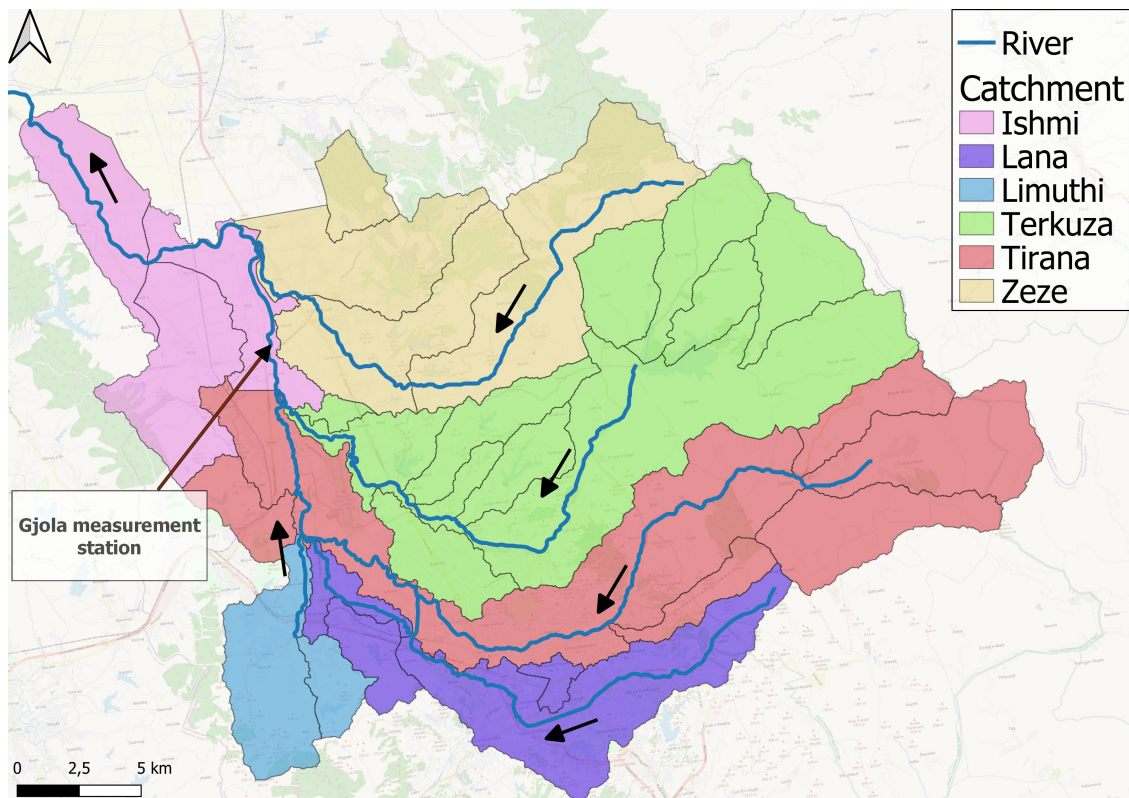


Figure 4.2: Sub-catchments areas

Table 4.4: Catchment area ratio

<b>Riverbasin</b>	<b>Area [<math>km^2</math>]</b>	<b>Ratio [%]</b>	<b>Hard coverage [%]</b>	<b>Effective contributing area [<math>km^2</math>]</b>	<b>Scaled ratio [%]</b>
Lana	64.66	14.1	52.5	36.39	20.4
Tirana	169.31	36.8	17.3	65.49	36.8
Terkuzi	193.78	42.1	7.2	65.09	36.5
Limuthi	32.26	7.0	9.0	11.12	6.2
<b>Total</b>	<b>460.0</b>				

Table 4.5: Discharges tributary per return period [ $m^3/s$ ]

<b>Return period [1/T]</b>	<b>Lana</b>	<b>Tirana</b>	<b>Terkuzi</b>	<b>Limuthi</b>
5	140.7	253.2	251.6	43.0
10	167.1	300.8	298.9	51.1
25	200.5	360.9	358.7	61.3
50	225.3	405.6	403.1	68.9
100	250.0	449.9	447.1	76.4
250	282.4	508.2	505.1	86.3

#### 4.4. Construction of HAND map

The outline of the procedure to generate inundation maps using height above nearest drainage was discussed in section 3.2.2. The first step is to hydrologically condition the DEM by pit removal. This ensures that each raster cell is able to drain to the end of the extent. The pit removal is performed with the TauDEM plugin for Arcmap initially and later with GRASS GIS. Additionally the flow in 8 directions is calculated and a flow direction map is produced. To derive the streams in the research area, also the flow accumulation can be calculated. The streams that are derived are sensitive to the chosen threshold and can therefore cause differences compared with the EU-Hydro river network dataset.

Since the EU-Hydro river network dataset is derived directly from the 25m DEM it is aligned with the pit removed DEM. Therefore instead of deriving streams through flow accumulation, the EU-Hydro river network is rasterized directly.

Now using the D-infinity distance down function in TauDEM, for each raster cell the vertical distance to the rasterized EU-Hydro stream network can be calculated. A visualization of this process is shown in figure 4.3.

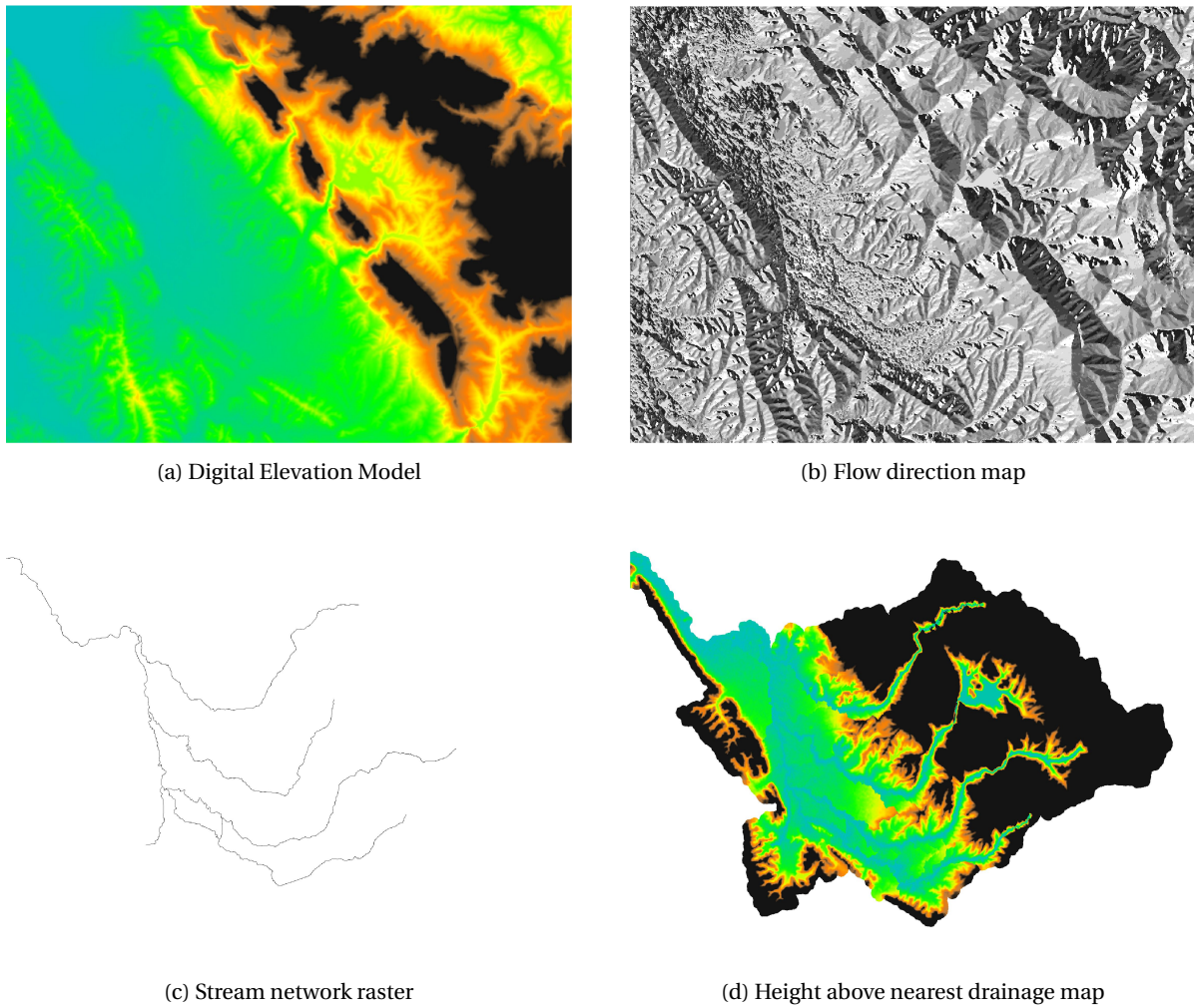


Figure 4.3: HAND map generation visualization

## 4.5. Synthetic rating curve development

In section 3.2.2 the method of Zheng et al. (2018) is introduced to generate a synthetic rating curve. To be able to describe damages and risk per sub-catchment, the complete procedure needs to be repeated for each sub-catchment to derive a sub-catchment specific SRC.

First the HAND map is clipped by each sub-catchment in figure 4.2. This results in a HAND map per sub-catchment and a mask is created. Additionally each mask is assigned with a value and incrementally increased from 0 to 4 with a step size of 0.5, corresponding to an inundation depth in meters. Now for each sub-catchment the inundation depth is derived by subtracting the HAND map from the mask layer. If a cell remains positive, it indicates inundations, all negative cells are set to 0. With the use of Zonal Statistics in Qgis the number of inundated cells and the total flood volume could be obtained. For each reach the slope is calculated through the DEM and Manning coefficients are estimated based on the state of the river, later explained in section 4.6. This forms the input for the method of Zheng et al. (2018) to develop the synthetic rating curve.

The following set of equations is solved for each sub-catchment and each stage between 0 and 4m:

$$d(s, y) = y - h(s), s \in F(y) \quad (4.7)$$

Water depth  $d(s, y)$  in cell  $s$  at reach-average water depth  $y$  is derived by subtracting the HAND value for each cell  $h(s)$  from the reach-average water depth. Positive values indicate the inundated zone  $F(y)$

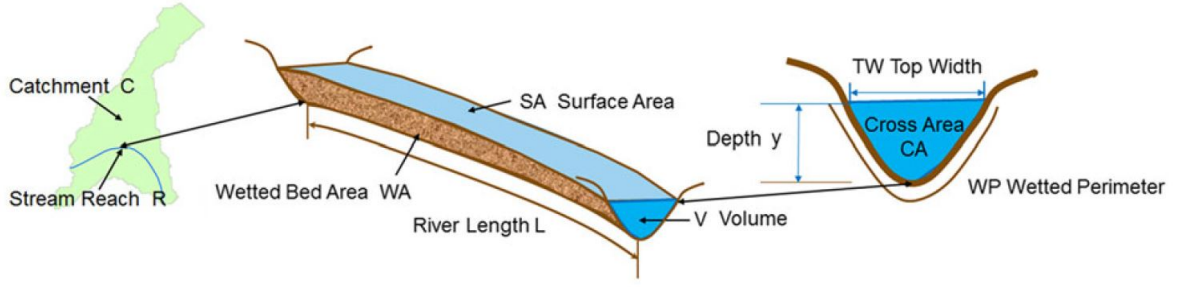


Figure 4.4: HAND river geometry (Zheng et al., 2018)

$$S(y) = \sum_{s \in F(y)} A(s) \quad (4.8)$$

Water surface area  $S(y)$  at depth  $y$  of the inundated zone described by the area  $A(s)$  of the inundated cells

$$B(y) = \sum_{s \in F(y)} A(s) \sqrt{1 + slp(s)^2} \quad (4.9)$$

Channel bed area  $B(y)$  of the inundated zone, with  $slp(s)$  as the surface slope.

$$V(y) = \sum_{s \in F(y)} A(s) d(s, y) \quad (4.10)$$

Flood volume  $V(y)$  of the inundated zone at water depth  $y$ .

$$W(y) = S(y)/L \quad (4.11)$$

Reach-average channel width, where  $L$  is the reach length.

$$A(y) = V(y)/L \quad (4.12)$$

Reach-average cross sectional area  $A(y)$

$$P(y) = B(y)/L \quad (4.13)$$

Reach-average wetted perimeter  $P(y)$

$$R(y) = A(y)/P(y) \quad (4.14)$$

Reach-average cross-sectional hydraulic radius  $R(y)$

$$Q(y) = \left(\frac{1}{n}\right) AR^{\frac{2}{3}} S^{\frac{1}{2}} \quad (4.15)$$

With the slope  $S$  for the reach and the Manning coefficient,  $n$ , the discharge  $Q(y)$  can be calculated.

Equations 4.7 - 4.15 result in a discharge related to the reach-average water depth. By plotting these values the synthetic rating curve is obtained. For the investigated catchments this led to unrealistic SRC's, where at low discharges below the bank-full discharge, inundation already occurred. It is concluded that the 25m resolution DEM was not able to capture the geometry of the river accurate enough. The geometry of the cross section through the HAND map is only able to capture the vertical location to the top of the river bank, but does not describe the river bed itself. Therefore a vertical shift to the SRC has to be made. Essentially this indicates that the method of Zheng et al. (2018) only describes the flood discharges in the investigated area and does not consider the discharge within the river bed.

To correct the SRC, first the discharge within the river bed is calculated. Then the flood discharge calculated with equations 4.7 - 4.15 is superimposed on the river bed discharge. This leads to a total discharge connected to an inundation level of the catchment. To calculate the river bed discharge the river geometry is assumed to

be trapezoidal and dimensions are estimated based on site visits, satellite images and distance calculations in Qgis. In the city centre of Tirana the Lana river is channelised and maintained significantly better than the more downstream reach. Therefore the river is divided into two different sections to increase the accuracy, see figure 4.5. The small branch of the Lana river is not considered in the SRC calculations because due to local development this branch is disconnected from the main channel. The discharges for each return period from table 4.5 are read from the SRC and thereby inundation stages are connected to a return period. The stages are listed in table 4.6.

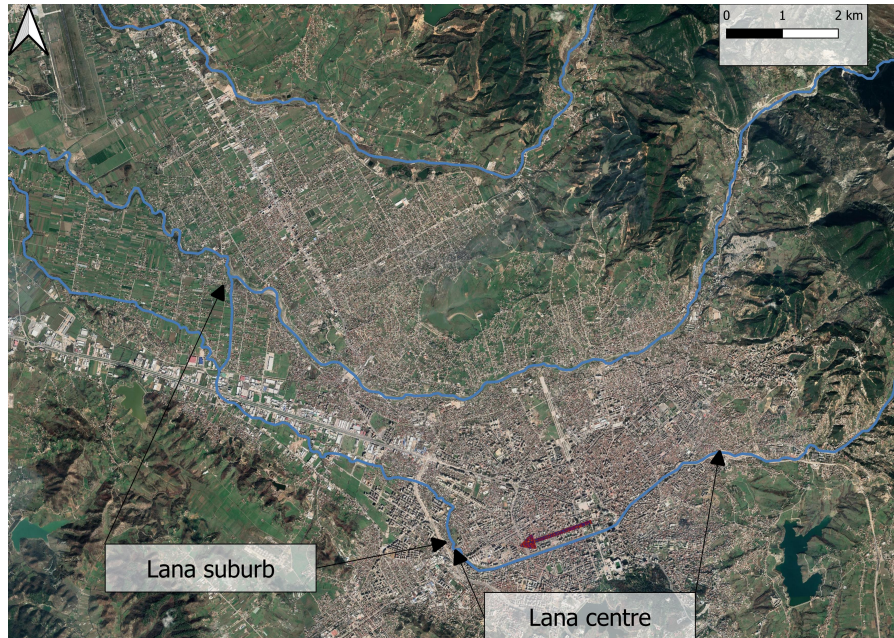


Figure 4.5: Division of Lana river, the arrows indicate the beginning and end of a section

Table 4.6: Inundation stages tributary per return period [m]

Return period [1/T]	Lana centre	Lana suburb	Tirana	Terkuzi	Limuthi
5	0.00	0.58	0.00	0.00	0.00
10	0.00	0.70	0.00	0.00	0.50
25	0.00	0.83	1.15	1.24	0.93
50	0.42	0.90	1.55	1.63	1.08
100	0.62	0.96	1.87	1.97	1.23
250	0.82	1.03	2.16	2.31	1.40

## 4.6. Manning coefficient estimation

In figure 4.6 the flood extent mapping from Copernicus (2017) Emergency Management Service is compared with the incrementally increasing inundation maps derived in section 4.5. The event has a return period estimated at 100 years (BRIGAID, 2017). The Manning coefficient is derived by an initial assumption which is later fine-tuned by visual comparison with the flood map.

First it was visually determined that the flooding event corresponds with a modelled flood with an inundation depth of 2.5m. From table 4.3 it is known that the discharge corresponding to a return period of 100 years is  $1223 \text{ m}^3/\text{s}$ . With these two parameters a single point on the synthetic rating curve is determined. Subsequently the Manning coefficient is altered in the equations 4.7 - 4.15 such that a discharge of  $1223 \text{ m}^3/\text{s}$  corresponds to an inundation stage of 2.5m. Through this procedure a Manning coefficient of 0.05 for the floodplain of the Ishmi river and 0.03 for the river bed was determined.



Several remarks about the modelled extent compared to the flood extent mapping have to be made. The Zeze catchment, indicated in figure 4.6b, is not considered in the flood risk assessment due to a lack of data. However, the mapped flood extent overlays both catchments. For visualization the Zeze is included, but marked in red to indicate the exclusion. For the purpose of visualization also a stage of 2.5 meter is selected for the Zeze, as could be expected for the most downstream part of the Zeze due to the backwater effect of joining the Ishmi river. Especially the area between Luz and Derven provides an accurate extent when 2.5m is assumed.

On the north bank of the Ishmi, Zone 1 in figure 4.6b, a small overestimation is observed. In this area local flood protection is present in the form of a levee. This levee forms the boundary to an agricultural area north of the Ishmi river. With the 25 meter resolution of the DEM this levee is not captured with high enough accuracy. Areas with strong anthropogenic interventions are not well captured with this terrain based approach. Zone 1 is therefore excluded from the visual fine-tuning.

The area in the south-west of the river, Zone 2 in figure 4.6b, is not modelled according to the observed extent. Additional investigation of the HAND map reveals that the flow direction in this area is directed at the Ishmi river further downstream, and not the shortest horizontal distance to the river (figure 4.6c). This results in a local ridge and plateau with higher values in the HAND map, causing that the area is not inundated. Even at higher inundation depths (>6m) this area will not inundate using the HAND method, therefore this area is not considered in the fine-tuning.

According to Chow (1959) Manning coefficients of 0.03 correspond to "clean, straight, full stage, no rifts or deep pools" channels. This is consistent with the average cross-section of the Ishmi river. A Manning coefficient of 0.05 is relatively rough and corresponds with "scattered brush, heavy weeds" or "light brush and trees, in winter". This is valid for a section of the floodplain. However, at higher inundation depths the influence of the roughness is expected to decrease.

## 4.7. Summary of hydraulic & risk parameters

In table 4.7 a complete overview of the input parameters to produce inundation and risk maps is presented. An important parameter is the current flood protection level. Without flood protection levels the entire damage-probability curve would be incorporated in the risk calculation. As is seen in figure 2.2b a section of the damage-probability curve can be corrected corresponding to the flood protection level. Therefore an approximation of local measures has to be made to produce a more realistic risk profile.

In the workshop the flood protection level was estimated at T=50 years. This corresponds to the reach of the Lana river in the city centre, where with well maintained banks inundation indeed only occurs after discharges corresponding to T=50 years. For other sections and rivers the banks are in poor maintained state and the protection level is estimated less than T=50 years. Nootenboom (2015) used a protection standard of 10 years in his assessment for the complete Balkan area. However, his dataset did not cover specific information of Albania and a minimum of 10 years was estimated for areas without data. As could be seen in figure 4.6 some local protection is present. Therefore, for the other catchments an average protection level of T=25 years is estimated.

The Manning coefficients for the Ishmi river are considered as a validated starting point for the other rivers. Based on the state of the river and banks, Manning coefficients are chosen in relation to the Ishmi coefficient values.

Table 4.7: Hydraulic &amp; risk parameters per catchment

<b>Parameter</b>	<b>Ishmi</b>	<b>Lana centre</b>	<b>Lana suburb</b>	<b>Tirana</b>	<b>Terkuzi</b>	<b>Limuthi</b>
L [m]	20,680	2,300	8,300	12,215	6,000	4,850
H [m]	16.8	13.0	42.7	65.0	6.5	24.9
A [ $m^2$ ]	240.00	47.25	28.00	105.00	120.00	16.00
S [-]	0.000814	0.00565217	0.00513976	0.005321	0.001083	0.005138
n - bed [-]	0.03	0.02	0.03	0.04	0.025	0.03
n - plain [-]	0.05	0.03	0.05	0.06	0.04	0.05
Protection standard [yr]	25	50	25	25	25	25

# 5

## Results

### 5.1. Results of risk calculation

#### 5.1.1. Inundation maps

For each return period the inundation maps are plotted and presented in figure 5.2. The area west of the Ishmi river is prone to the highest inundation depths. The area is a plain enclosed by a mountain ridge and the Ishmi river. In the centre of Tirana it can be observed that no inundation occurs for return periods up to 50 years. For return periods higher than 50 years inundation on the south bank of the Lana river takes place. The suburban surroundings of the Lana are prone to inundation at lower return periods. The Limuthi river, although with relatively low discharges, shows inundation at a commercial site and large shopping centre. Along the Tirana river inundation starts at T=25 year at multiple sites. These areas are known for informal housing with often little flood protection. The Terkuzi catchment is less prone to inundation. The inundation at higher return periods mainly occurs outside of the residential areas.

The accuracy of the inundation zone is determined by comparison of the modelled extent and the observed extent. Only for the Ishmi catchment an observed inundation is available, for which the accuracy is calculated. The extent is not directly modelled but visually identified and fine-tuned as explained in section 4.6. Johnson et al. (2019) defined the accuracy as:

$$\text{Accuracy} = \frac{\text{True wet area}}{\text{True wet area} + \text{False dry area} + \text{False wet area}} \quad (5.1)$$

In figure 5.1 for the Ishmi catchment the correct modelled area, the underpredicted area and the overpredicted area are visualized. Based on this figure equation 5.1 results in:

$$\text{Accuracy} = \frac{850 \text{ ha}}{850 \text{ ha} + 439 \text{ ha} + 735 \text{ ha}} = 42\% \quad (5.2)$$

The calculated accuracy includes the areas that could not be captured due to limitations in the DEM and HAND map. These limitations were explained in section 4.6 and reflect on the accuracy of 42%. These specific or other limitations were not found in the more upstream catchments.

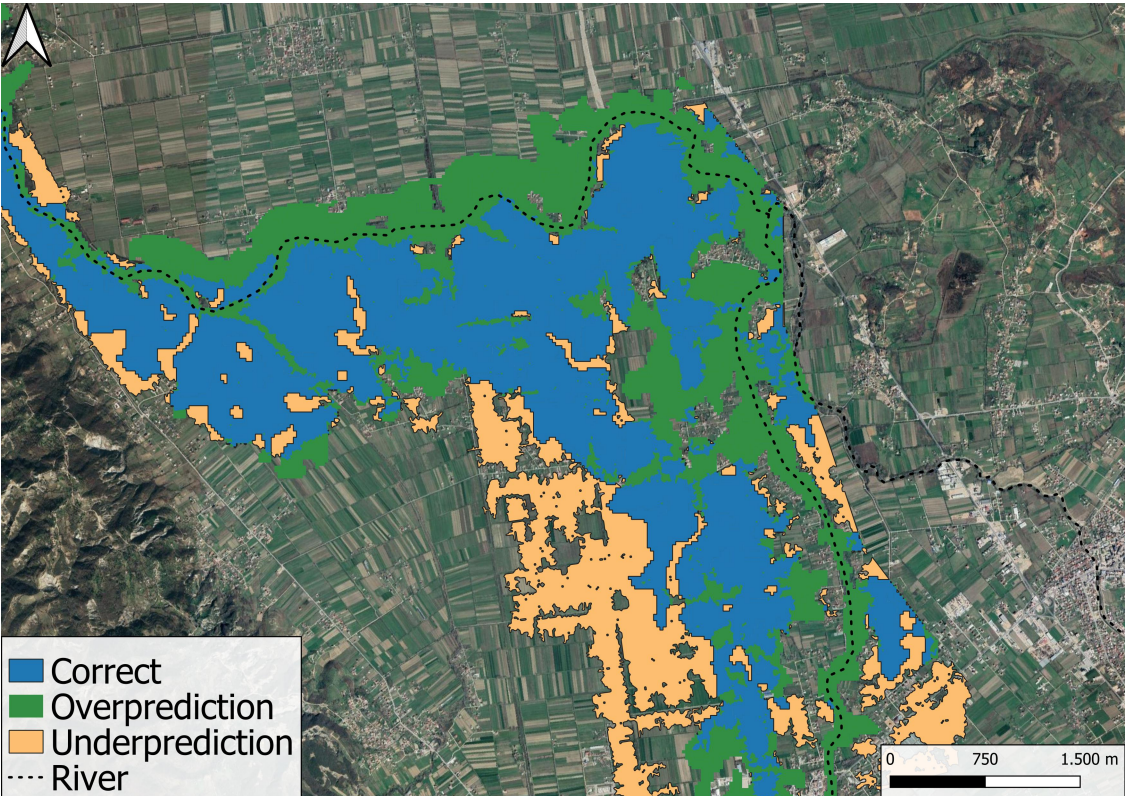
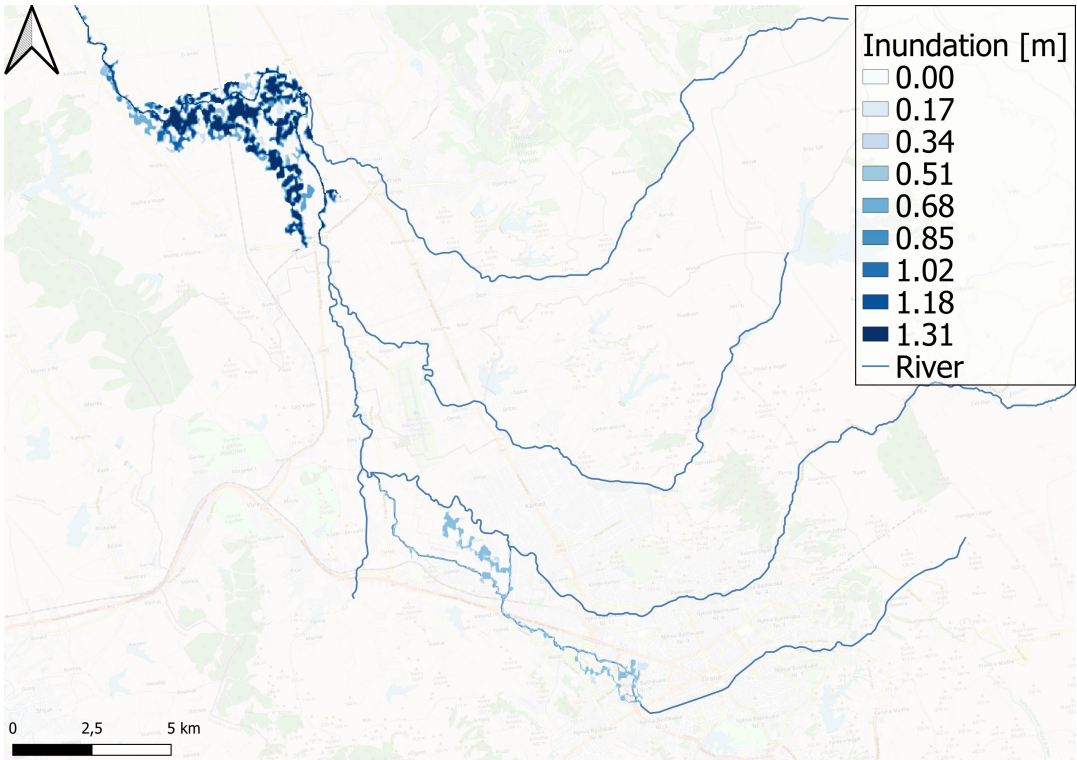
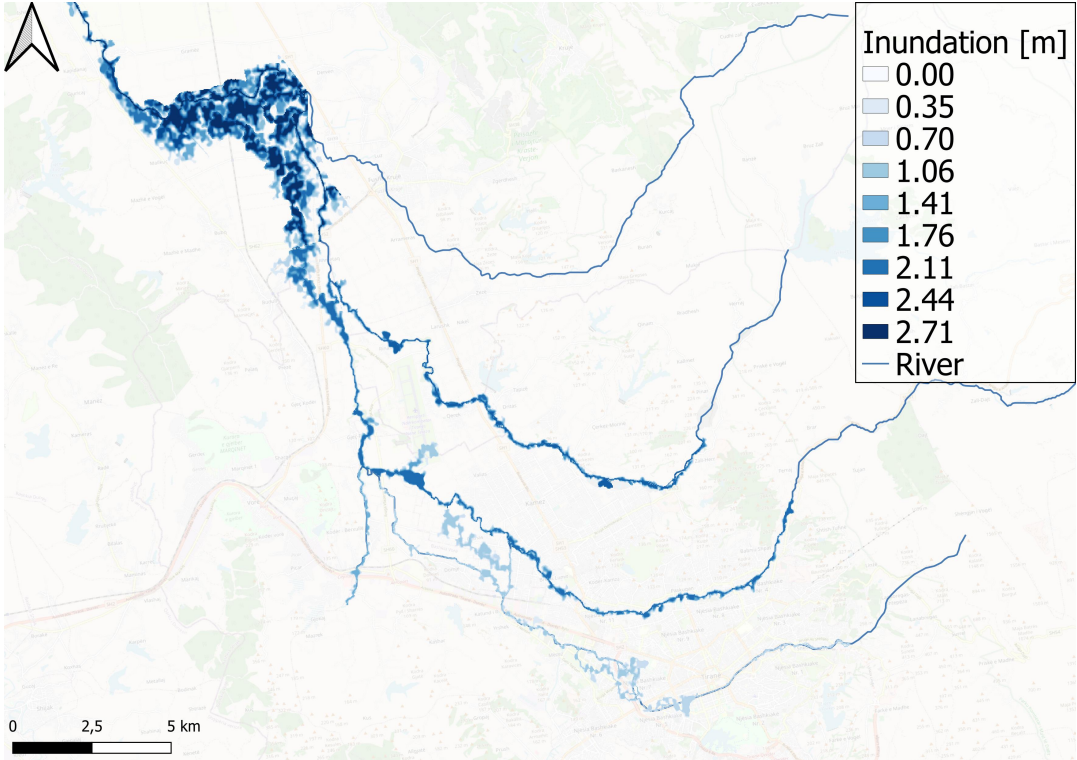


Figure 5.1: Accuracy of inundation map at Ishmi catchment



(a) T= 5 yr



(b) T= 250 yr

Figure 5.2: Inundation maps per return period

### 5.1.2. Damage-probability curves

In figure 5.3 the damage-probability curves are presented. With these curves the risk expressed in expected annual damage (EAD) can be calculated. For all areas the damages are also listed in table 5.1.

Table 5.1: Damage and risk overview

Return period [1/T]	Lana Centre [M€]	Lana Suburb [M€]	Tirana [M€]	Terkuzi [M€]	Ishmi[M€]	Limuthi [M€]
0	0.0	0.0	0.0	0.0	0.0	0.0
5	0.0	17.6	0.0	0.0	14.1	0.0
10	0.0	22.2	0.0	0.0	21.9	1.6
25	0.0	28.0	31.8	0.3	30.0	3.4
50	8.5	31.3	47.0	0.4	34.8	4.2
100	12.4	34.1	60.3	0.6	39.0	5.0
250	16.5	37.5	73.8	0.8	44.3	6.0
<b>EAD [€]</b>	<b>148,742</b>	<b>852,443</b>	<b>1,396,122</b>	<b>12,915</b>	<b>967,850</b>	<b>120,400</b>

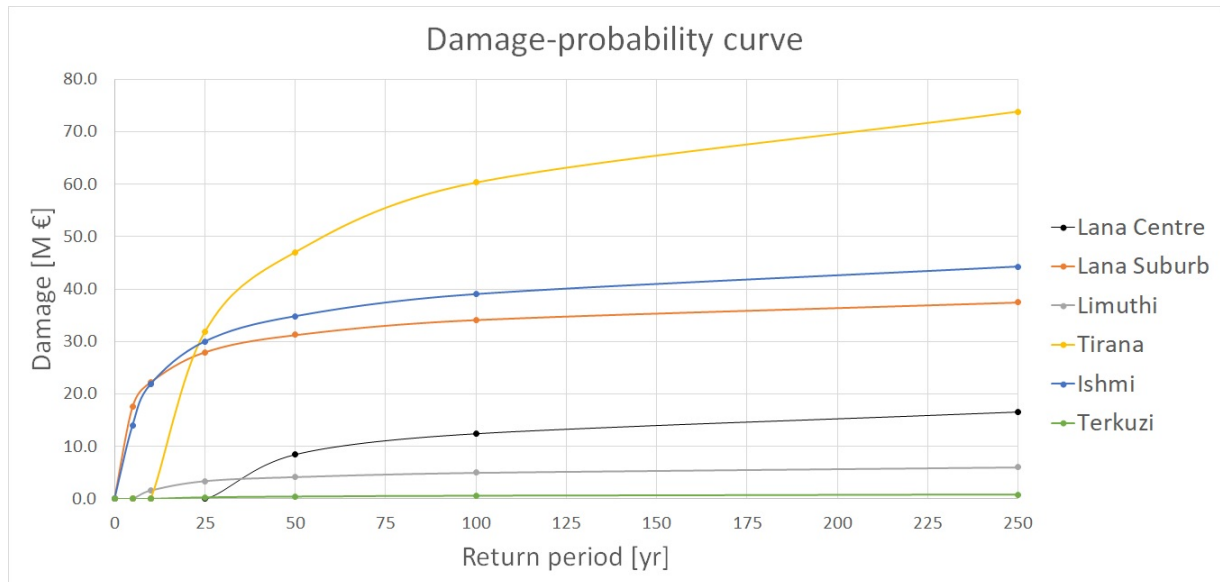


Figure 5.3: Damage-probability curve

From the damage-probability curve in figure 5.3 it can be observed that both the Lana Suburb reach and the Ishmi river have a steep curve for low return periods. In terms of absolute damages the Tirana catchment receives the most damages and also the highest expected annual damage. It must be noted that damages and EAD are calculated over the complete area of the catchment. Therefore, for a direct comparison of the risk per catchment the area should be included. If the EAD is divided by the area, the Lana catchment has the highest risk with an EAD of 15,483 Euro per km<sup>2</sup> compared to the Tirana catchment with 8,245 Euro per km<sup>2</sup>, making it a factor 1.8 more susceptible in terms of EAD.

## 5.2. Risk map

In figure 5.4 the risk map for the entire Ishmi basin is presented, based on the damage-probability curve and taken into consideration flood protection levels. Several residential areas are identified. Furthermore a risk hotspot can be seen at the location of the City Park shopping mall. This risk area is consistent with the 2017 flooding event where people were evacuated from the shopping mall. Finally across the entire Tirana and Lana river several hotspots are seen. This area is presented in figure 5.5 in more detail. The commercial area along the main road was also affected in the 2017 flood event.

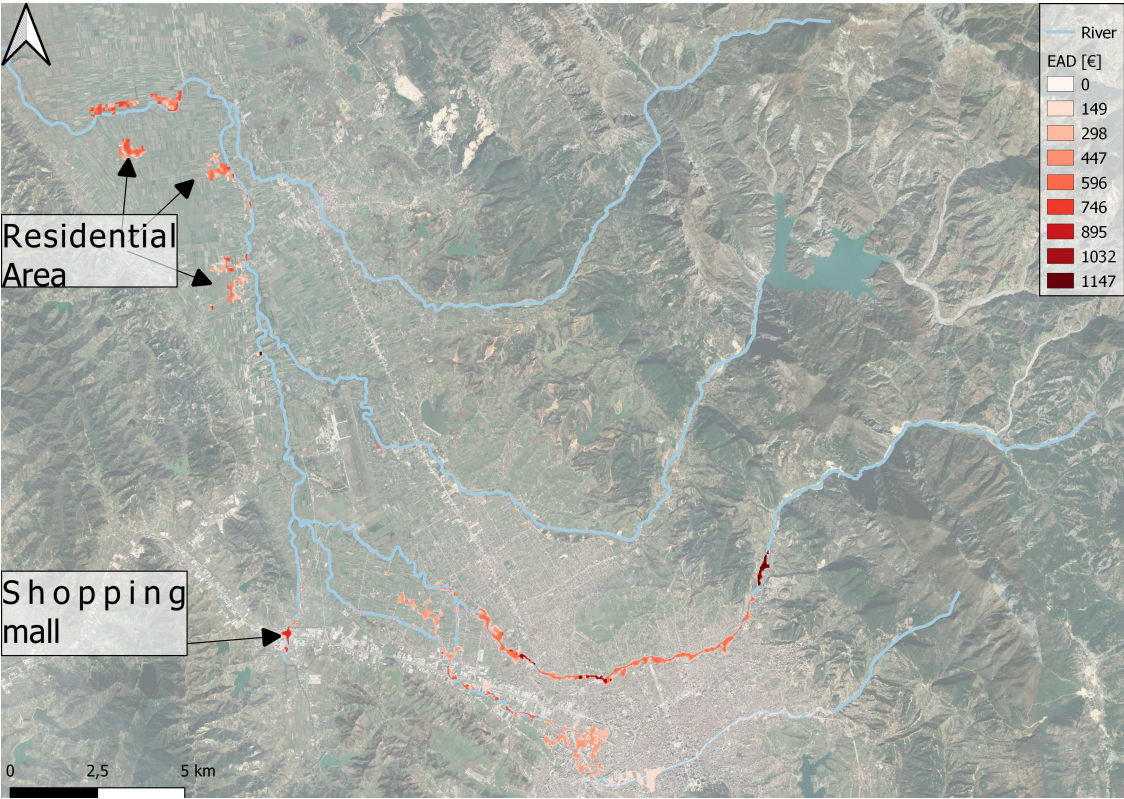


Figure 5.4: Risk map Ishmi basin

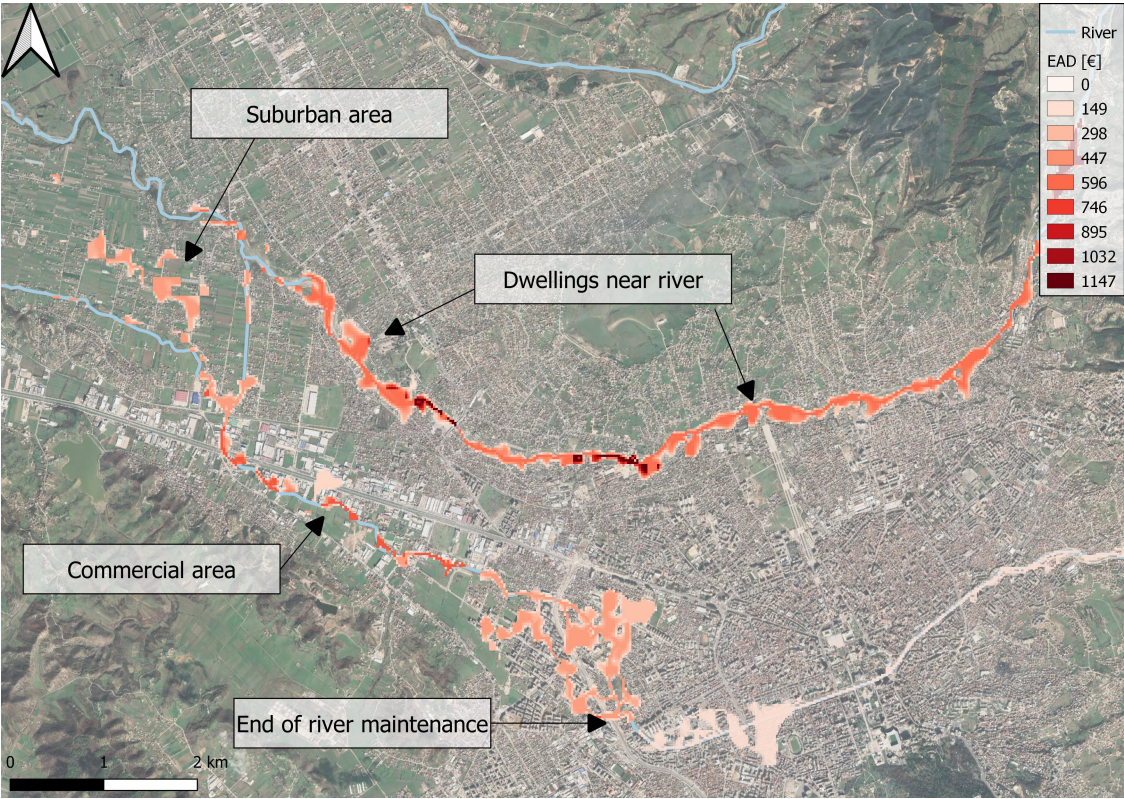


Figure 5.5: Risk map Lana & Tirana catchment

### 5.3. Flood risk reduction

In this section the effect on damages and flood risk of the proposed measures as discussed in section 1.1 are presented. The sub-group of the workshop focussed mainly on the suburban Lana river section. Also in section 5.1.2 it is concluded that the Lana river has the highest EAD value per area. Therefore the reduction measures will only be focussed on the suburban Lana river section. To translate the proposed measures to the flood risk assessment the following approach is followed, where for each measure a new synthetic rating curve will be derived to compute the flood risk:

- Model waste removal and bank improvement through incremental decrease of roughness coefficient.
- Model modified cross-section through an increase of the cross-sectional area.
- Include above measures in a future projection including intensive urbanization.

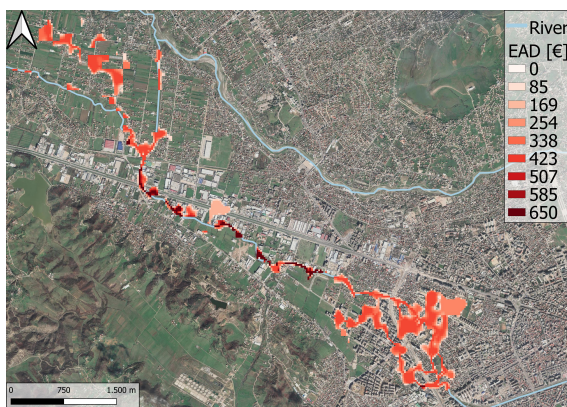
#### 5.3.1. Waste removal and bank improvement

As seen in figure 1.4 waste aggregation imposes a negative influence on the hydraulic capacity of the river. Furthermore bank maintenance is in poor shape for large stretches of the river. One of the conceptual measures is to remove waste and sediment from the riverbed by dredging and to improve riverbanks. From a hydraulic perspective this indicates a lower Manning coefficient corresponding to a smoother riverbed and banks. In table 5.2 the effect of a decrease in Manning coefficient is seen. First the coefficient for the riverbed itself is lowered, then the coefficients for the floodplain are lowered. For reduction measure 5 the Manning coefficients are similar to the well maintained section in the city centre. A reduction in expected annual damage of 338,029 Euro is seen with RD5, corresponding to 39.7%.

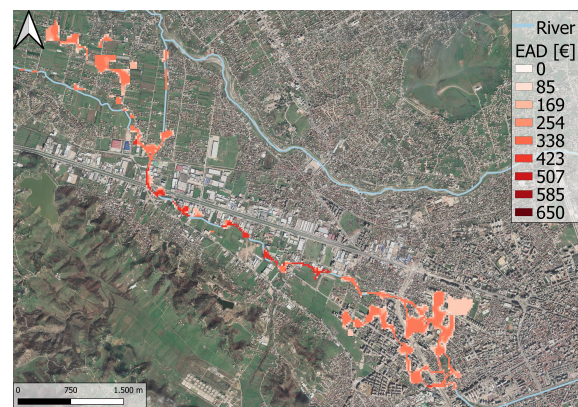
In figure 5.6 it can be observed that the risk extent is significantly less intruding in the commercial area along the main road. This also indicates that less indirect damage is expected through disruption of traffic.

Table 5.2: Flood risk riverbed and bank improvement

Measure	Manning bed [-]	Manning plain [-]	EAD [€]	Reduction [€]	Reduction [%]
Current	0.03	0.05	852,443	-	-
RD1	0.025	0.05	793,985	58,458	6.9
RD2	0.02	0.05	689,900	162,543	19.1
RD3	0.03	0.04	749,485	102,958	12.1
RD4	0.03	0.03	642,481	209,962	24.6
RD5	0.02	0.03	514,414	338,029	39.7



(a) Risk Lana suburb no measures



(b) Risk Lana suburb measure RD5

Figure 5.6: Risk comparison riverbed and bank improvement

### 5.3.2. Modified cross-sectional area

In the workshop a multifunctional cross-section, with higher discharge capabilities at peak flow conditions was proposed. This measure is approximated through an increase of the area of the cross-section of the river. Included in this measure is an improvement of riverbed and banks. The dimensions are based on the cross-sectional area of the Lana river in the city centre. In table 5.3 an overview of the calculated risk is presented and the corresponding risk map is shown in 5.7. The EAD is decreased with 549,788 Euro, which is a reduction of 64.5%. An additional reduction in extent of the risk can be observed.

Table 5.3: Flood risk modified cross-sectional area

Measure	Cross-sectional area [ $m^2$ ]	Manning bed [-]	Manning plain [-]	EAD [€]	Reduction [€]	Reduction [%]
Current	28.00	0.03	0.05	852,443	-	-
RD6	47.25	0.02	0.03	302,655	549,788	64.5%

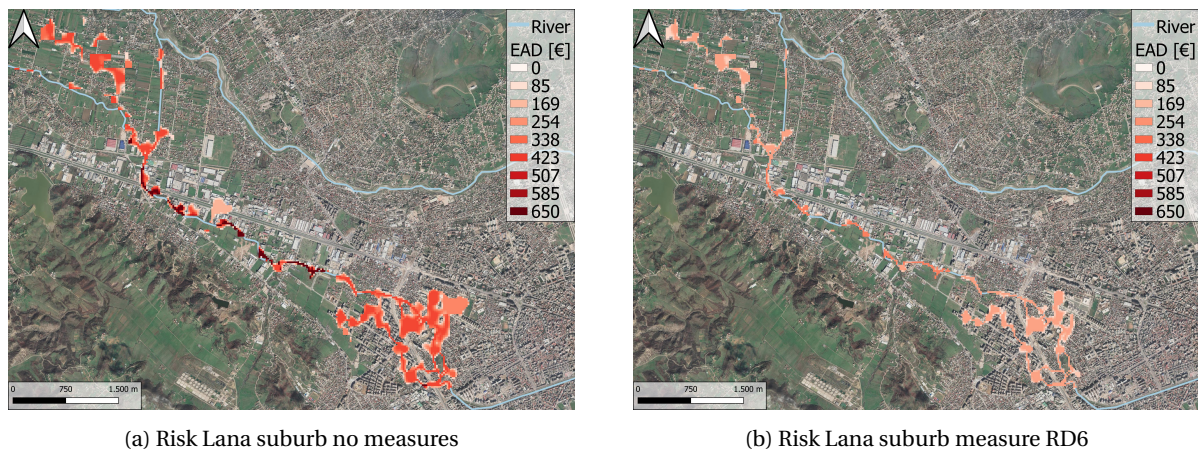


Figure 5.7: Risk comparison multifunctional cross-section

### 5.3.3. Future urbanization projection

The suburban area of the Lana river is due to its relatively flat area an ideal location for future expansion of the city. However, building in the flood plain will impose an increase in flood risk. To simulate the effect of future urbanization and the potential effect of reduction measures, the land use map is changed accordingly. In figure 5.8 it can be observed that several areas in the Lana catchment are currently marked as agriculture areas. In the future urbanization scenario these patches of agricultural area will be assumed to be fully transformed into residential areas.

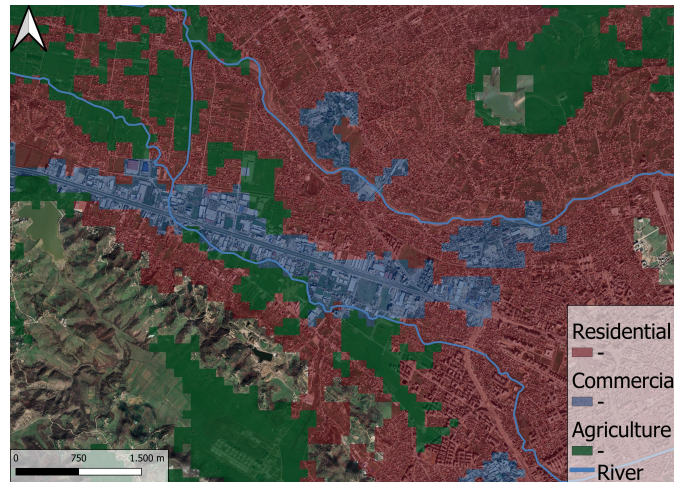
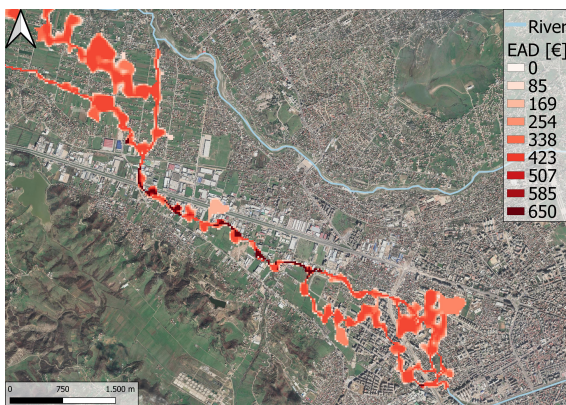


Figure 5.8: Current land use Lana catchment

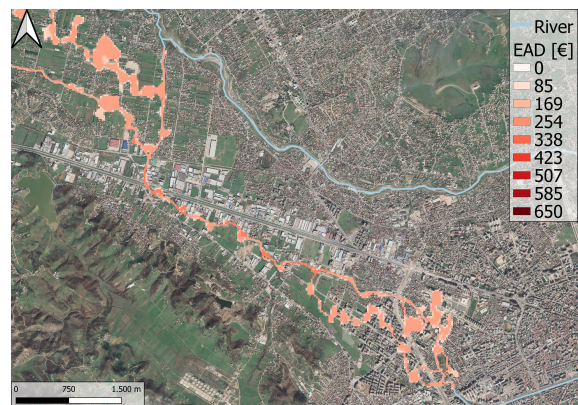
In table 5.4 the current flood risk, future flood risk and the implementation of the reduction measure from section 5.3.2 is shown. A risk map is presented in figure 5.9. Without additional measures an increase in flood risk of 84% can be expected. When measures are included this expected risk can then be reduced by 62%. Thereby the possible reduction of RD6 is increased to €978,078, making the measure more economically viable. Also visually it can be determined from figure 5.9 that a clear increase in risk is present in former agricultural areas.

Table 5.4: Flood risk overview future urbanization

Situation	EAD [€]
Current	852,443
Urbanization - no measures	1,570,852
Urbanization - with measure RD6	592,774



(a) Urbanization - no measures



(b) Urbanization - with measure RD6

Figure 5.9: Flood risk under influence urbanization

# 6

## Discussion and limitations

The calculated risk is based on the product of hazard, exposure and vulnerability, each with their own assumptions and implications. To assess the quality of the risk assessment and to interpret the results properly, the sources for the assessment and results are discussed. First the quality of the data is addressed, secondly the steps and calculations to process the data are reviewed and finally the relevance of the results is discussed.

### 6.1. Data sources

The land use information from Copernicus (2017) is considered a reliable source, with a reported total reliability of 87% (European Environment Agency, 2006). For the commercial, industrial and continuous urban fabric class over 95% reliability is achieved. However, the resolution of the dataset is only 100 meter. To be compatible with the other data sources the raster is re-sampled to 25 meter. Despite this, the dataset is a limiting factor in terms of resolution and defines the eventual risk assessment to be set at a 100 meter accuracy. Other data sources like OpenStreetMap (OSM) can provide higher accuracy, but often have lower reliability due to data gaps (Kosters, 2015; Van der Veer, 2015; Suijkens, 2015). A hybrid version for the land use maps could be opted, where OSM information is leading and the data gaps are filled with Copernicus (2017). Also for transferability to a global setting the use of OSM could prove to be useful.

In terms of vulnerability, maximum damages and European depth-damage functions per land use class have been used. The use of general functions for a specific region remains a rough estimation. In addition the function is normalized and might not describe actual present flooding mechanisms and characteristics of the region. As described by Wagenaar et al. (2016) the epistemic uncertainty is high with the use of depth-damage functions and it is expected to be of importance in the Tirana area. In the Tirana river catchment more informal housing is present, compared to the city centre, with often no flood protection. Aliaj (2002) describes the development of 4,500 dwellings in this area, in the period 1989-1994, where 50% of the population resided. The majority of these dwellings are built without permits and have poor infrastructure. In more developed neighbourhoods more resources are available for private measures. More area specific depth-damage functions, obtained through local damage reports, could capture potential damage mechanism differences between areas more accurate. Furthermore the damage values are given on a national level, but do not take into account regional differences based on GDP per capita. An approach where regional GDP per capita information is included could provide a higher accuracy. The option is available in FIAT, but no distinguishable GDP information is present within the extent of the case study.

Assumptions in current flood protection levels have a significant impact in the risk assessment. In this thesis flood protection levels were estimated per catchment, based on the intended flood protection standards. An additional study in the safety level and failure probability of current flood protection could provide a more accurate representation of the actual flood protection level in the region.

## 6.2. Data processing review

An important source for the approach in this thesis is the discharge information in the area. The most recent year with measurements was 1992 and the dataset might not capture current maximum discharges, since no climate change scenario was taken into consideration. Due to data constraints, only one dataset for one measurement location, downstream in the basin, was obtained. In section 4.3 the discharges at the Gjola station were used to obtain information about the tributaries. Given the total area of the catchments of the tributaries (460km<sup>2</sup>) and the mountainous character of the region, spatial variability is expected. However, since the major flooding events investigated occur after long rainfall events, the spatial distribution is expected to be more homogeneous at this temporal scale. Datasets for each tributary would provide a more veracious assessment, however, the current approach was found to be acceptable given the purpose of the assessment. To substantiate this statement the modelled inundation at the Lana river in the city centre matched the expected flood protection standard, which is an indication that the used discharges are within the same order of magnitude. A final remark has to be made about reservoirs in the area. In the upstream catchment of the Terkuzi river an embankment dam reservoir is present that acts as the drinking water supply for Tirana. The maximum storage capacity of the reservoir is  $80 \times 10^6 \text{ m}^3$  with a drainage area of approximately 98km<sup>3</sup> (Miho et al., 2009). The construction was finished in 1996 and therefore the potential effect on discharges is not captured in the used dataset. Given the total basin area of 705 km<sup>3</sup>, impact of the reservoir is expected and inclusion in a future assessment is advisable.

The HAND map that is generated forms the geographic source of the inundation extent. Before generating the HAND map, pit removal of the DEM is of importance to ensure that each pixel will drain to the end of the extent, without being enclosed in local depressions. The pit removal procedure essentially smooths the surface of the DEM. Dependent on the algorithm and/or software tool that is used, differences in the extent of the HAND map can occur. With TauDEM an overestimation of the potential inundation zone can be seen in figure 6.1. The HAND map proves to be sensitive in flat areas with anthropogenic intervention, due to the geographic error introduced by pit removal. This is consistent with findings of Zheng et al. (2018) and Johnson et al. (2019) who state that the method is more accurate in areas with more gradient where "the flood routing process is controlled by the topographic setting". Review of the HAND map with local knowledge remains important, in which the extent should be validated by comparison with the actual drainage area. This ensures that no areas are assumed connected to the river, that in the actual situation are disconnected, as described in figure 6.1.

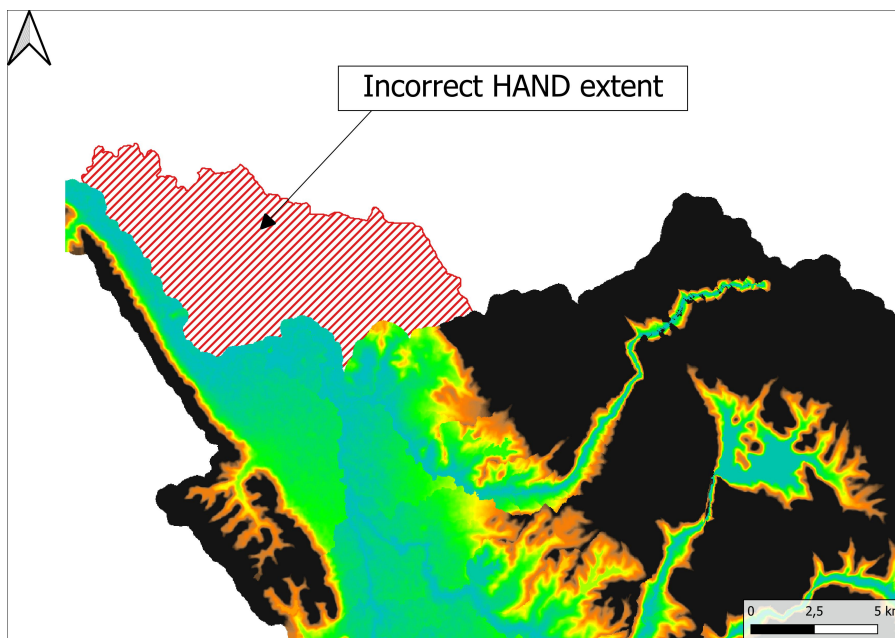


Figure 6.1: HAND map generated with GRASS GIS & TauDEM in red

In the synthetic rating curve development the geometry of the river is described. The most dominant assumption is the use of an uniform depth for the entire reach and reach averaged geometries. Increased accuracy can be achieved when longer reaches are split in multiple sections. Regarding the roughness coefficients in the original method of Zheng et al. (2018), a single Manning coefficient is used. In their discussion a compound uniform flow is opted, where the river bed is separated from the floodplain to better match the hydraulics. In this thesis this distinction was made, since the coarser 25m DEM could not provide any river bed geometry information. In hindsight the approach can be seen as an unexpected improvement. By computing the river bed discharge a shift was imposed on the rating curve and for the current region this provided a better approximation. When the HAND inundation mapping is used with coarser DEM's, local knowledge about river geometry should be included.

Although the distinction between channel and floodplain can be seen as an improvement, single coefficients for these two remain an estimation. A more accurate description of the roughness can be obtained with composite roughness estimation. The Horton-Einstein is opted by Tullis (2012) as the most favourable method to obtain the composite Manning coefficient. This would provide a better estimation for flow processes in the inundated zone. Johnson et al. (2019) found that varying the Manning coefficients in all tested sites lead to correct discharges and Zheng et al. (2018) states that a correct calibration of the Manning coefficient leads to "near-real water depth prediction". However, it is highly dependant on the use case of the assessment if the additional effort of composite roughness estimation has to be made. Zheng et al. (2018) found that within the scope of "regional-scale estimation" and "approximate inundation mapping" no significant improvement of the flood extent was seen despite the extra effort. Consistent with these studies, the results in this thesis are less sensitive to the Manning coefficient than river bed geometries. This is demonstrated by the risk reduction measures, where the reduction of risk with a larger cross-section was a factor 1.6 higher compared to the measure with lower Manning coefficients only. These findings indicate that the current approach regarding the Manning coefficients is acceptable given the purposes of this thesis, with the caveat that results of the assessment should be interpreted accordingly.

The total inundation map is achieved by adding the inundation of the reaches together in one map. Thereby it is assumed that flooding and water depth in the rivers are independent of each other. However, in the investigated area backwater effects at river joints can be expected, leading to higher than modelled water depths. In addition, the Lana river is divided in two sections where the more downstream section has significantly less hydraulic capacity. Also within a section itself a backwater effect is to be expected. In the particular case of the Lana river the bad maintained shape of the suburban section will most likely have negative effects in the city centre. The used method does not allow for the inclusion of these effects. The accuracy for the Ishmi catchment was 42%. In the study of Johnson et al. (2019) a mean accuracy of 19% was found over 28 floodplains, also without consideration of backwater. It is difficult to compare the accuracy of the inundation mapping since the accuracy of 42% does not reflect the accuracy of modelling, but merely indicates the best possible fit that was visually achieved. For other areas no accuracy could be computed, due to the lack of mapped flood extents. However, the computed high risk areas match with reports of flooding. In addition the accuracy of 42% was obtained in a relatively flat area, where accuracy can be expected to be lower, making it encouraging for the sloping upstream area where the city centre is located. Currently the 25m DEM proved to be too coarse for direct use, but future development in the available datasets could provide an increase in accuracy. Hawker et al. (2018) names the MERIT and TanDEM-X products as potential successor to the currently popular SRTM DEM. In addition Hawker et al. (2018) describes the process of "editing or stochastic simulation of existing DEM data" to improve flood simulation.

Finally an important benefit of the method is that the computational effort and procedures are relatively simple to perform. The procedures to obtain synthetic rating curves and inundation maps can easily be scripted in Python. Computational time for this extent is estimated in the order of under a minute to produce a full set of inundation maps for each return period. In addition, the computational time of FIAT is around 1 minute to compute a complete risk profile and damages, including GIS ready maps. The high accessibility and high technical transferability of the method is a significant benefit.

### **6.3. Risk assessment interpretation**

The inundation and risk map matches reports of areas where damages and risk occurred and captures the local character in the urban area of Tirana. Taken into account the technical limitations and constraints, the method added benefit in the phase of conceptual design. Especially in the short time frame of the workshop in Tirana, the method could have provided important insights and could have helped to substantiate the proposed measures. The risk reduction quantification of the measures provides direct insight in the effects. Although direct adoption of damage values and annual expected damage should be done carefully, the impact of interventions can be meaningfully interpreted when focussed on the relative reduction.

The Ishmi catchment suffers largest inundation extents and several hotspots are identified in the risk map. The identification of this area underlines the added benefit of the assessment. In the workshop, described in section 1.1, little attention was focussed on the area, but this assessment highlighted the importance by revealing a bottleneck in the drainage system. The proposed measures are focussed on improved drainage capacity upstream, which could lead to adverse effects in the Ishmi catchment, such as increased frequency of flooding and increased inundation depths. In addition, the land use map indicated a large agricultural area. Improvement from a flood risk perspective in the Ishmi area through better drainage could lead to water shortages for the agricultural sector during dry periods. These insights are beneficial in the phase of conceptual interdisciplinary designs.

# 7

## Conclusions

Global economic losses due to flooding have increased over the past decades. Albania is an example of a country that has experienced an increase in flooding frequency and economic losses in the last 20 years. In 2017 the capital city Tirana faced the largest flooding event in history. The identification of areas with high flood risk is important to create awareness at public and private level. For the Tirana area, conceptual designs to reduce flood risk were developed in a student workshop in May 2018. Quantification of the flood risk reduction of these conceptual designs can support decision making in early stages. However, currently data availability often limits the applicability of flood risk assessment methods in urban areas such as Tirana. Therefore, first a flood risk assessment method applicable in areas with poor or scarce data needed to be identified and secondly this method was applied to the Tirana area with a risk reduction quantification of the conceptual designs.

The identified method used to assess flood risk expresses the risk in Expected Annual Damage (EAD) in Euro and identifies river flooding only and no local pluvial flooding. It consist of the product of hazard, exposure and vulnerability and estimated flood protection levels. For the exposure component residential, commercial, infrastructure and agriculture land use classes and maximum damage values are used. The vulnerability is expressed through European depth-damage functions per land use class. The hazard component is an inundation map with inundation depth in meters. This inundation map is generated by a Height Above Nearest Drainage (HAND) map in combination with a Synthetic Rating Curve (SRC). The SRC is generated through the application of the Manning equation for reach-averaged geometries, derived from the HAND map and computed for inundation stages from 0 to 4m.

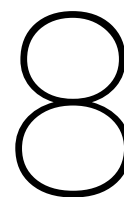
The method was applicable in the Tirana area and benefits are the low computational requirements and straightforward GIS operations. This imposes opportunities for transferability to other regions with scarce data. All procedures can easily be scripted in the Python language code and computational time for the investigated extent is in the order of minutes.

The HAND based hazard mapping revealed limitations in data quality and accuracy. The European Digital Elevation Model (DEM) with a 25 meter resolution proved to be too coarse to capture river geometry for direct use in the SRC development. Local knowledge of river geometry therefore remains important to describe the inundation process and needs to be manually included. In addition the possible inundation extent was found to be sensitive due to the pit removal process in flat areas. In areas with more gradient the inundation extent is expected to have a higher accuracy. Judgement of the generated HAND map with local knowledge is needed and in the absence of more detailed DEM's the method is more applicable for small extents where this effort of manual intervention is viable. In general the hazard estimation is based on a simplification of the flooding hydraulics and geometries, making the assessment applicable for indicative purposes. Within the scope of decision making and design in the conceptual phase, the method adds benefit.

Several high risk areas were identified and in terms of absolute risk the Tirana catchment scored the highest risk. However, if the area of the catchment is taken into consideration, the Lana catchment scored highest with a risk, defined in Expected Annual Damage (EAD), of approximately one million Euro. This was mainly caused by poor maintenance of the most downstream part of the river, which contributed to 85% of the risk in the area. Several smaller risk hotspots were also identified that match reported areas during the flood of

2017. Finally, for a significant agricultural area with several settlements in the Ishmi catchment, a risk of just under one million Euro was computed. Despite the limitations and assumptions of the method, meaningful identification of areas was possible.

Flood risk reduction measures could easily be modelled. A multifunctional cross-section was most effective with a reduction of 65%. A less intensive measure such as bank improvement led to a reduction of 40%. Although the exact values are difficult to interpret directly, relative comparison formed an adequate guidance. The need for measures was clearly demonstrated by an urbanization scenario in which the flood risk increased with 84% and thereby also the gains of the multifunctional cross-section increased. The assessment of measures in an early stage can help to direct and guide in the conceptual stages of interdisciplinary design. In addition the assessment revealed the potential adverse effect of upstream measures on other areas and underlined the importance of an integral approach.



## Recommendations

- To verify the accuracy, it is advised to perform the method in an area with more available data about discharges, discharge-stage relationships, inundation extent and inundation depth.
- For a more verifiable area, it would provide valuable insight to compare the method with a DEM of different resolutions. It is expected that a coarse DEM leads to less accuracy. A direct comparison could quantify the differences and place this research in better perspective.
- The fine-tuning of the Manning coefficient was performed visually. An improved procedure, with the calculated accuracy of the extent as leading factor, could increase the accuracy of the risk assessment.
- It is highly recommended to develop a Python script of all GIS procedures and risk calculations.
- For the case study it is advised to improve the discharge data with a more recent dataset, which includes the constructed reservoir and captures climatic changes of the past 30 years.

# Bibliography

- Aliaj, B. *Governing cities: NGOs/CBOs and housing for low-income people in Albania*, pages 109–128. 12 2002. ISBN 978-1-85339-497-3. doi: 10.3362/9781780441177.
- Bogdani, M. and Selenica, A. Catastrophic floods and their "risk" in the rivers of albania. *National Institute of Hydrometeorology*, 1997.
- BRIGAUD. Tirana short report on water, sewage, energy, waste and road network. *Field investigation report*, 2017.
- Chow. Reference tables for manning's n values for channels. [http://www.fsl.orst.edu/geowater/FX3/help/8\\_Hydraulic\\_Reference/Mannings\\_n\\_Tables.htm](http://www.fsl.orst.edu/geowater/FX3/help/8_Hydraulic_Reference/Mannings_n_Tables.htm), 1959. Accessed: 30-05-2021.
- CIA. The world factbook. <https://www.cia.gov/the-world-factbook/countries/albania/>, 2021. Accessed: 20-02-2021.
- Copernicus. Emsr258: Flood in albania. <https://emergency.copernicus.eu/mapping/list-of-components/EMSR258>, 2017. Accessed: 18-05-2021.
- Davies, R. Albania – calls for international help after floods damage homes and infrastructure. <http://floodlist.com/europe/albania-floods-damage-december-2017>, 2017. Accessed: 10-02-2021.
- European Environment Agency. The thematic accuracy of corine land cover 2000. *EEA Technical report, 7/2006*, 2006. URL [https://land.copernicus.eu/user-corner/technical-library/technical\\_report\\_7\\_2006.pdf](https://land.copernicus.eu/user-corner/technical-library/technical_report_7_2006.pdf).
- Field, C., Barros, V., Stocker, T., Qin, D., Dokken, D., Ebi, K., Mastrandrea, M., Mach, K., Plattner, G., and Allen, S. Managing the risks of extreme events and disasters to advance climate change adaptation. a special report of working groups i and ii of the intergovernmental panel on climate change. *IPCC*, 2012.
- Hawker, L., Bates, P., Neal, J., and Rougier, J. Perspectives on digital elevation model (dem) simulation for flood modeling in the absence of a high-accuracy open access global dem. *Frontiers in Earth Science*, 6:233, 2018. ISSN 2296-6463. doi: 10.3389/feart.2018.00233. URL <https://www.frontiersin.org/article/10.3389/feart.2018.00233>.
- Huizinga, J. Flood damage functions for eu member states. *Technical report, JRC - Institute for Environment and Sustainability*, 2007.
- Huizinga, J., Moel, H. d., and Szewczyk, W. Global flood depth-damage functions. methodology and the database with guidelines. *EUR 28552 EN*, 2017. doi: 10.2760/16510.
- Institute of Hydrometeorology. Discharges gjola station. *Republic of Albania*, 1992.
- Johnson, J. M., Munasinghe, D., Eyelade, D., and Cohen, S. An integrated evaluation of the national water model (nwm)–height above nearest drainage (hand) flood mapping methodology. *Natural Hazards and Earth System Sciences*, 19(11):2405–2420, 2019. doi: 10.5194/nhess-19-2405-2019. URL <https://nhess.copernicus.org/articles/19/2405/2019/>.
- Jonkman, S. Global perspectives on loss of human life caused by floods. *Natural Hazards and Earth System Sciences*, 34:151–175, 2005.
- Jonkman, S. Loss of life estimation in flood risk assessment. *PhD Dissertation Delft University of Technology*, 2007.
- Jonkman, S., Jorissen, R., Schweckendieck, T., and Van den Bos, J. Lecture notes flood defences cie5431, 2017.
- Kosters, A. Flood risk assessment for urban areas in asia. *Bachelor Thesis Delft University of Technology*, 2015.

- Kron, W. Flood risk = hazard • values • vulnerability. *Water International*, 30:58–68, 2005. doi: 10.1080/02508060508691837. URL <https://doi.org/10.1080/02508060508691837>.
- Lushaj, B., Hoxhaj, F., Ndini, M., Selenica, A., Pambuku, A., Dafa, I., Hasimi, A., Zaimi, K., Marku, M., Como, E., Vako, E., Isufaj, S., and Myrtaj, B. General overview of the transboundary waters of rivers, lakes, groundwater and trend of them, in albania. *Online International Interdisciplinary Research Journal*, 2011.
- Merz, B., Kreibich, H., Schwarze, R., and Thielen, A. Review article "assessment of economic flood damage". *Natural Hazards and Earth System Sciences*, 10(8):1697–1724, 2010. doi: 10.5194/nhess-10-1697-2010. URL <https://nhess.copernicus.org/articles/10/1697/2010/>.
- Messner, F., Penning-Rowsell, E., Green, C., Meyer, V., Tunstall, S., and Van der Veen, A. Evaluating flood damages: guidance and recommendations on principles and methods. *FLOODsite*, 2007.
- Miho, A., Shuka, L., Cullaj, A., and Bachofen, R. Environmental analyses of bovilla watershed (albania) - an overview. 2009.
- Munich Reinsurance Company. *NatCatSERVICE Database*, 2013.
- Nootenboom, T. Global flood risk index for urbanized areas near rivers. *Internship Report Wageningen University & Research*, 2015.
- PBL. Navigating rivers and deltas towards a sustainable future. <https://themasites.pbl.nl/future-water-challenges/river-basin-delta-tool/understanding-the-system/projected-trends/>, 2021. Accessed: 25-02-2021.
- Selenica, A., Kuriqi, A., and Ardicioglu, M. Risk assessment from floodings in the rivers of albania. *International Balkans Conference on Challenges of Civil Engineering*, 2011.
- Slager, K., Burzel, A., Bos, E., de Bruijn, K., Wagenaar, D., Winsemius, H., Bouwer, L., and van der Doef, M. User manual delft-fiats version 1. 2017.
- Suijkens, S. Identifying delta regions most vulnerable for flooding, a multiple land use flood risk assessment for australia. *Bachelor Thesis Delft University of Technology*, 2015.
- Tapsell, S. M., Penning-Rowsell, E. C., Tunstall, S. M., and Wilson, T. L. Vulnerability to flooding: Health and social dimensions. *Philosophical Transactions: Mathematical, Physical and Engineering Sciences*, 360(1796):1511–1525, 2002.
- Toto, E. and Massabo, M. Historical collection of disaster loss data in albania. *CIMA Research foundation*, 2014.
- Tullis, B. Hydraulic loss coefficients for culverts. *NCHRP*, 734, 2012. URL <https://www.nap.edu/read/22673/chapter/1>.
- Van Beek, L. and Bierkens, M. The global hydrological model pcr-globwb: Conceptualization, parameterization and verification. *Report Department of Physical Geography, Utrecht University, The Netherlands*, 2008. URL <http://vanbeek.geo.uu.nl/suppinfo/vanbeekbierkens2009.pdf>.
- Van Berchum, E. C., Mogley, W., Jonkman, S. N., Timmermans, J. S., Kwakkel, J. H., and Brody, S. D. Evaluation of flood risk reduction strategies through combinations of interventions. *Journal of Flood Risk Management*, 12(S2):e12506, 2019. doi: <https://doi.org/10.1111/jfr3.12506>. URL <https://onlinelibrary.wiley.com/doi/abs/10.1111/jfr3.12506>.
- Van Berchum, E. C., van Ledden, M., Timmermans, J. S., Kwakkel, J. H., and Jonkman, S. N. Rapid flood risk screening model for compound flood events in beira, mozambique. *Natural Hazards and Earth System Sciences*, 20(10):2633–2646, 2020. doi: 10.5194/nhess-20-2633-2020. URL <https://nhess.copernicus.org/articles/20/2633/2020/>.
- Van der Pol, T., van Ierland, E., and Gabbert, S. Economic analysis of adaptive strategies for flood risk management under climate change. *Mitigation and Adaptation Strategies for Global Change*, 22, 03 2015. doi: 10.1007/s11027-015-9637-0.

- Van der Veer, M. Flood risk assessment for south-american cities. *Bachelor Thesis Delft University of Technology*, 2015.
- Verkade, J. S. and Werner, M. G. F. Estimating the benefits of single value and probability forecasting for flood warning. *Hydrology and Earth System Sciences*, 15(12):3751–3765, 2011. doi: 10.5194/hess-15-3751-2011. URL <https://hess.copernicus.org/articles/15/3751/2011/>.
- Verschuur, J. Flood risk evaluation and smart flood risk city management. *Master Thesis Delft University of Technology*, 2016.
- Wagenaar, D. J., de Bruijn, K. M., Bouwer, L. M., and de Moel, H. Uncertainty in flood damage estimates and its potential effect on investment decisions. *Natural Hazards and Earth System Sciences*, 16(1):1–14, 2016. doi: 10.5194/nhess-16-1-2016. URL <https://nhess.copernicus.org/articles/16/1/2016/>.
- Ward, P., Jongman, B., Sperna Weiland, F., Bouwman, A., Van Beek, R., Bierkens, M., Ligtoet, W., and Winsemius, H. Assessing flood risk at the global scale: model setup, results, and sensitivity. *Environmental Research Letters*, 8(4):044019, oct 2013. doi: 10.1088/1748-9326/8/4/044019. URL <https://doi.org/10.1088/1748-9326/8/4/044019>.
- Ward, P., Jongman, B., Aerts, J., Bates, P. D., Botzen, W., Diaz Loaiza, A., Hallegatte, S., Kind, J. M., Kwadijk, J., Scussolini, P., and Winsemius, H. A global framework for future costs and benefits of river-flood protection in urban areas. *Nature Climate Change*, 7(9):642–646, 2017. ISSN 1758-6798. doi: 10.1038/nclimate3350. URL <https://doi.org/10.1038/nclimate3350>.
- Winsemius, H. C., Van Beek, L. P. H., Jongman, B., Ward, P. J., and Bouwman, A. A framework for global river flood risk assessments. *Hydrology and Earth System Sciences*, 17(5):1871–1892, 2013. doi: 10.5194/hess-17-1871-2013. URL <https://hess.copernicus.org/articles/17/1871/2013/>.
- Worldbank. Gdp per capita. <https://data.worldbank.org>, 2021. Accessed: 20-02-2021.
- Zheng, X., Tarboton, D. G., Maidment, D. R., Liu, Y. Y., and Passalacqua, P. River channel geometry and rating curve estimation using height above the nearest drainage. *JAWRA Journal of the American Water Resources Association*, 54(4):785–806, 2018. doi: <https://doi.org/10.1111/1752-1688.12661>. URL <https://onlinelibrary.wiley.com/doi/abs/10.1111/1752-1688.12661>.